



1 Attaining Whole-Ecosystem Warming Using Air and Deep Soil 2 Heating Methods with an Elevated CO₂ Atmosphere

3
4 Paul J. Hanson^{1*}, Jeffery S. Riggs², W. Robert Nettles¹, Jana R. Phillips¹, Misha B. Krassovski¹,
5 Leslie A. Hook¹, Lianhong Gu¹, Andrew D. Richardson³, Donald M. Aubrecht³, Daniel M.
6 Ricciuto¹, Jeffrey M. Warren¹ and Charlotte Barbier⁴

7
8 ¹Climate Change Science Institute, Oak Ridge National Laboratory, Oak Ridge, Tennessee, USA.

9 ²Integrated Operations Support Division, Oak Ridge National Laboratory, Oak Ridge, Tennessee, USA.

10 ³Harvard University, Cambridge, Massachusetts, USA.

11 ⁴Instrument and Source Division, Oak Ridge National Laboratory, Oak Ridge, Tennessee, USA.

12
13 *Correspondence to: P. J. Hanson, e-mail: hansonpj@ornl.gov, tel. 1-865-574-5361

14
15 Notice: This manuscript has been authored by UT-Battelle, LLC under Contract No. DE-AC05-00OR22725 with the
16 U.S. Department of Energy. The United States Government retains and the publisher, by accepting the article for
17 publication, acknowledges that the United States Government retains a non-exclusive, paid-up, irrevocable, world-
18 wide license to publish or reproduce the published form of this manuscript, or allow others to do so, for United
19 States Government purposes. The Department of Energy will provide public access to these results of federally
20 sponsored research in accordance with the DOE Public Access Plan ([http://energy.gov/downloads/doe-public-](http://energy.gov/downloads/doe-public-access-plan)
21 [access-plan](http://energy.gov/downloads/doe-public-access-plan)).

22
23 **Abstract.** This paper describes the operational methods to achieve and measure both deep soil
24 heating (0-3 m) and whole-ecosystem warming (WEW) appropriate to the scale of tall-stature,
25 high-carbon, boreal forest peatlands. The methods were developed to allow scientists to provide
26 a plausible set of ecosystem warming scenarios within which immediate and longer term (one
27 decade) responses of organisms (microbes to trees) and ecosystem functions (carbon, water and
28 nutrient cycles) could be measured. Elevated CO₂ was also incorporated to test how temperature
29 responses may be modified by atmospheric CO₂ effects on carbon cycle processes. The WEW
30 approach was successful in sustaining a wide range of above and belowground temperature
31 treatments (+0, +2.25, +4.5, +6.75 and +9 °C) in large 115 m² open-topped chambers with
32 elevated CO₂ treatments (+0 to +500 ppm). Air warming across the entire 10 enclosure study
33 required ~90% of the total energy for WEW ranging from 64283 MJ d⁻¹ during the warm season
34 to 80102 MJ d⁻¹ during cold months. Soil warming across the study required only 1.3 to 1.9 % of
35 the energy used ranging from 954 to 1782 MJ d⁻¹ of energy in the warm and cold seasons,
36 respectively. The residual energy was consumed by measurement and communications systems.
37 Sustained temperature and elevated CO₂ treatments were only constrained by occasional high
38 external winds. This paper contrasts the in situ WEW method with closely related field warming
39 approaches using both above (air or infrared heating) and belowground warming methods. It also
40 includes a full discussion of confounding factors that need to be considered carefully in the



41 interpretation of experimental results. The WEW method combining aboveground and deep soil
42 heating approaches enables observations of future temperature conditions not available in the
43 current observational record, and therefore provides a plausible glimpse of future environmental
44 conditions.
45



46 1. Introduction

47 Measurements through time and across space have shown that the responses of terrestrial
48 ecosystems to both chronic and acute perturbations of climatic and atmospheric drivers can lead
49 to changes in ecosystem structure (e.g., species composition, leaf area, root distribution; IPCC
50 2014, Walther et al. 2002, Cramer et al. 2001) and ecosystem function (e.g., plant physiology,
51 soil microbial activity, and biogeochemical cycling; Bronson 2008, 2009). The projected
52 magnitudes and rates of future climatic and atmospheric changes, however, exceed conditions
53 exhibited during past and current inter-annual variations or extreme events (Collins et al. 2013),
54 and thus represent conditions whose ecosystem-scale responses may only be studied through
55 manipulations at the field scale. Science working groups have focused on next generation
56 ecosystem experiments (Hanson et al. 2008) and concluded that there is “a clear need to resolve
57 uncertainties in the quantitative understanding of climate change impacts” and that “a
58 mechanistic understanding of physical, biogeochemical, and community mechanisms is critical
59 for improving model projections of ecological and hydrological impacts of climate change.”
60 Furthermore, a number of reviews have recently called for new studies of climate extremes
61 including experimental warming to obtain measurements for warming scenarios that go beyond
62 the observable records (Cavaleri et al. 2015; Kayler et al. 2015; Torn et al. 2015).

63

64 Consensus projections of the climatic and atmospheric changes from the Fifth Assessment
65 Report of the Intergovernmental Panel on Climate Change (IPCC) vary spatially across the
66 globe. Warming is, however, projected to be greatest at high latitudes with temperature increases
67 larger in winter than summer (Collins et al. 2013). A mean warming of as much as 2.6 to 4.8°C
68 during the summer and winter respectively is expected by the end of this century, based on GCM
69 calculations for the IPCC RCP8.5 scenario. That level of warming exceeds the typically
70 observed variation in mean annual temperatures ($\pm 2^\circ\text{C}$) and therefore represents a range of
71 conditions that necessitates experimental manipulation. In addition, future extreme summer heat
72 events may expose ecosystems to acute heat stress that exceed historical and contemporary long-
73 term conditions for which extant vegetation is adapted.

74

75 Warming has been studied using many methods in field settings with the most common methods
76 focused on warming low stature or juvenile vegetation and surface soils using infrared heaters,



77 small open top chambers or near-surface heating cables - all of which have restricted warming
78 capacities (Aronson and McNulty 2009). This paper describes warming methodologies that take
79 us to the other extreme: systems capable of producing warming at multiple temperature levels in
80 larger plots (>100 m²) and throughout the soil profile (depths well below 1 m) and above tall
81 vegetation. The methodology was initially demonstrated in a small 12 m² chamber (Hanson et al
82 2011), scaled up to a full-sized prototype >100 m² (Barbier et al. 2012), then deployed into a
83 black spruce – sphagnum peat bog in northern Minnesota as a platform for the Spruce and
84 Peatland Response Under Climatic and Environmental Change (SPRUCE) experiment
85 (<http://mnspruce.ornl.gov>; Krassovski et al. 2015)

86
87 SPRUCE was conceived to provide whole-ecosystem experimental treatments that span a wide
88 range of warming scenarios to improve understanding of mechanistic processes and
89 consequential ecosystem-level impacts of warming on peatlands. SPRUCE is evaluating the
90 response of existing *in situ* and tall-stature (>4 m) biological communities to a range of
91 temperatures from ambient conditions to +9°C for a *Picea mariana* (Mill.) B.S.P. [black spruce]
92 – *Sphagnum* spp. peatland forest in northern Minnesota. Because this ecosystem is located at the
93 southern extent of the spatially expansive boreal peatland forests it is considered to be especially
94 vulnerable to climate change, and warming is expected to have important feedbacks on the
95 atmosphere and climate through enhanced greenhouse gas emissions (Bridgman 2006; Davidson
96 and Janssens 2008; Strack et al. 2008). The primary goals of the research were 1) to test how
97 vulnerable an important C-rich terrestrial ecosystem is to atmospheric and climatic change, 2) to
98 test if warming of the entire soil profile would release large amounts of CO₂ and CH₄ from a
99 deep C-rich soil, and 3) to derive key temperature response functions for mechanistic ecosystem
100 processes that can be used for model validation and improvement. SPRUCE provides an
101 excellent opportunity to investigate how atmospheric and climatic change alter the interplay
102 between vegetation dynamics and ecosystem vulnerability, while addressing critical uncertainties
103 about feedbacks through the global C and hydrologic cycles.

104

105 This paper describes the operational methods applied to achieve both deep soil heating, or in this
106 case, deep *peat* heating (DPH), and whole-ecosystem warming (WEW) appropriate to the scale
107 of the 6-m tall boreal forest and underlying peat. While the primary goal for SPRUCE was to



108 focus on the response of a high-C peatland ecosystem to rising temperatures, elevated CO₂
109 (eCO₂) was also incorporated into the experimental design to test how the temperature response
110 surfaces may be modified by expected changes in atmospheric [CO₂]. The paper further
111 describes confounding factors that need to be considered carefully in the interpretation and
112 analysis of the experimental results (Leuzinger et al. 2015). While a comprehensive literature
113 comparison to other warming methods (Rustad et al. 2001; Shaver et al. 2000; Aronson and
114 McNulty 2009) was not an objective of this paper, the nature of the *in situ* WEW method is
115 discussed in the context of closely related field warming approaches deployed with both above
116 (air or infrared heating) and belowground warming methods.

117

118 **2. Methods**

119 **2.1 A brief discussion of the SPRUCE Experimental Infrastructure**

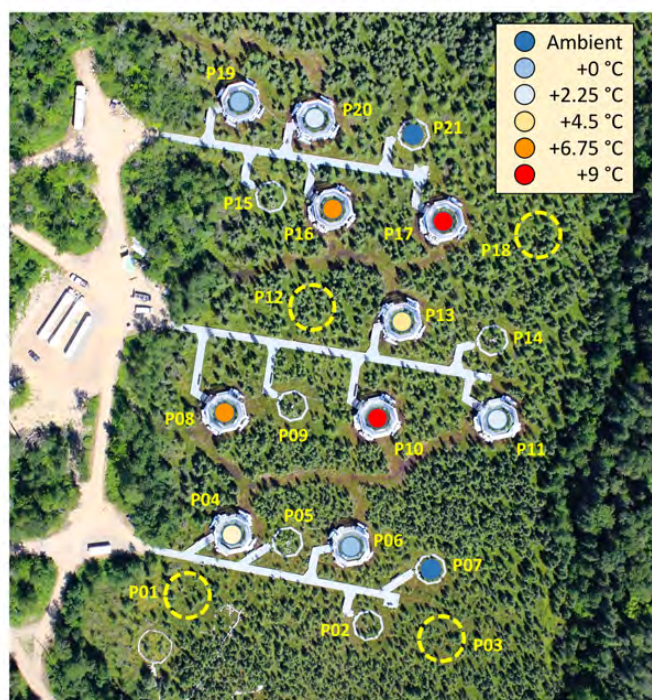
120 Experimental plots and infrastructure in support of the SPRUCE WEW study were established
121 on the S1-Bog of the Marcell Experimental Forest (MEF; Kolka et al. 2011). Raised boardwalks
122 were added in 2012, electrical and communication system were added in 2013, provisions for
123 belowground heating were added in 2014, and the aboveground enclosures and air warming
124 systems were added between January and June of 2015. Infrastructure for the addition of eCO₂
125 was added in 2016. Pretreatment data were collected throughout the 2012 to 2015 period.

126

127 An original plan for the SPRUCE experimental temperature and CO₂ treatments included a
128 traditional replicated ANOVA design, but a quantitative analysis of various experimental designs
129 and discussions among experimentalists and modelers led to the conclusion that a regression-
130 based experimental design (Cottingham et al. 2005) including a broad range of temperature
131 levels would yield long-term data more suited for the characterization of response curves for
132 application within ecosystem and earth system models (see also Kardol et al. 2012). If necessary
133 for some assessments of significance warming effects (e.g., individual tree growth), the
134 regression combination of treatment plots might be justifiably binned into low, medium and high
135 temperature treatments for ANOVA-based analyses. An important assumption underlying this
136 choice was that there were no strong gradients across the experimental area that would mandate a
137 block design. Preliminary survey data from the chosen site justify making this assumption (e.g.,
138 Parsekian et al. 2012; Tfaily et al. 2014).



139



140
141

142 **Figure 1:** Aerial photograph of the SPRUCE experimental site on August 5, 2015. Plot numbers
143 (1 to 21) and assigned temperature treatments are superimposed on the image. Dashed circles
144 indicated established plot centers for plots that are monitored annually for tree growth. Plots 4,
145 10, 11, 16 and 19 receive elevated CO₂. The middle boardwalk is 112 m long.

146

147 An aerial photograph of the SPRUCE site shows the random assignment of treatments to plots
148 (Fig. 1). Tfaily et al. (2014) and Krassovski et al. (2015) provide details for the experimental site,
149 which include three ~100 m transect boardwalks for accessing 17 octagonal permanent plots
150 over the southern half of the 8.1 ha bog. Electrical supply systems (for belowground heating and
151 instrumentation), propane vaporizers and delivery pipelines (for forced-air heating), pure CO₂
152 delivery pipelines (for eCO₂ additions), and a data communication network (Krassovski et al.
153 2015) were initially installed along each transect to serve the individual permanent plots. Ten of
154 the permanent plots were randomly assigned to the following warming treatments: 2 fully-
155 constructed control plots with no energy added (henceforth simply control plots), and 2 plots
156 each to be managed as +2.25, +4.5, +6.75 and +9 °C warming plots. Two unchambered ambient



157 plots are also part of the experimental design. Enclosure methods for warming of the air and
158 belowground peat are described further in the following sections.

159

160 Each of the ten plots is surrounded beneath the surface by a corral made of interlocking vinyl
161 sheet pile walls (Model ESP 3.1, EverLast Synthetic Products, LLC) for the hydrologic isolation
162 of each plot as an independent ombrotrophic system (Sebestyen and Griffiths 2016). Following
163 installation, each sheet piles extends above the bog surface approximately 0.3 m having been
164 driven vertically through the peat profile (3 to 4 m) into the underlying ancient lake sediment.
165 Slotted outflow pipes allow for lateral drainage and hydrologic measurements and sampling from
166 each plot. The operation and performance of the corral system will be described in a future
167 paper. During the period of performance covered in this manuscript, the bog remained very wet
168 with a water table near the surface.

169

170 **2.2 Site Description**

171 The climate of the MEF is subhumid continental, with large and rapid diurnal and seasonal
172 temperature fluctuations (Verry et al., 1988). Over the period from 1961 through 2005 the
173 average annual air temperature was 3.3 °C, with daily mean extremes of -38 °C and 30 °C, and
174 the average annual precipitation was 768 mm. Mean annual air temperatures have increased
175 about 0.4 °C per decade over the last 40 years (Sebestyen et al., 2011).

176

177 The investigated peatland is the S1-Bog of the MEF (N 47° 30.476'; W 93° 27.162' and 418 m
178 above mean sea level). The S1-Bog is an ombrotrophic peatland with a perched water table that
179 has little regional groundwater influence. The S1-Bog is dominated by *Picea mariana* (Mill.)
180 B.S.P. (black spruce) with contributions to the forest canopy from *Larix laricina* (Du Roi) K.
181 Koch (larch). The S1-Bog was harvested in strip cuts in 1969 and 1974 to test the effects of
182 seeding on the natural regeneration of *P. mariana*. In its current state of regeneration, the canopy
183 is 5-8 m tall. The peatland soil is the Greenwood series, a Typic Haplohemist
184 (<http://websoilsurvey.nrcs.usda.gov>) with average peat depths to the Wisconsin glacial-age lake
185 bed of 2 to 3 m (Parsekian et al., 2012). Recent surveys of the peat depth, bulk density, and C
186 concentrations for the S1-Bog suggest a total C storage pool of greater than 240 kgC m⁻²



187 (calculated to a 3 m average depth), with greater than 90% over 3000 years old (Karis
188 McFarlane, personal communication).

189

190 Vegetation within the S1-Bog is dominated by two tree species (see above), and is supported by
191 a bryophyte layer dominated by *Sphagnum* spp mosses, especially *S. angustifolium* and *S. fallax*
192 in hollows and *S. magellanicum* on drier hummocks. Other mosses including *Pleurozium* spp
193 (feather mosses) and *Polytrichum* spp (haircap mosses) are also present. The understory includes
194 a layer of ericaceous shrubs including *Rhododendron groenlandicum* (Oeder) Kron & Judd
195 (Labrador tea), *Chamaedaphne calyculata* (L.) Moench. (leatherleaf) with a minor component of
196 other woody shrubs. The bog also supports a limited number of herbaceous species including:
197 the summer-prevalent *Maianthemum trifolium* (L.) Sloboda (Three-leaf false Solomon's seal), a
198 variety of sedges (*Rhynchospora alba* (L.) Vahl, *Carex* spp.) and *Eriophorum vaginatum* (cotton
199 grass). The belowground peat profile and geochemistry are described in Tfaily et al. (2014).

200

201 **2.3 Air warming protocols**

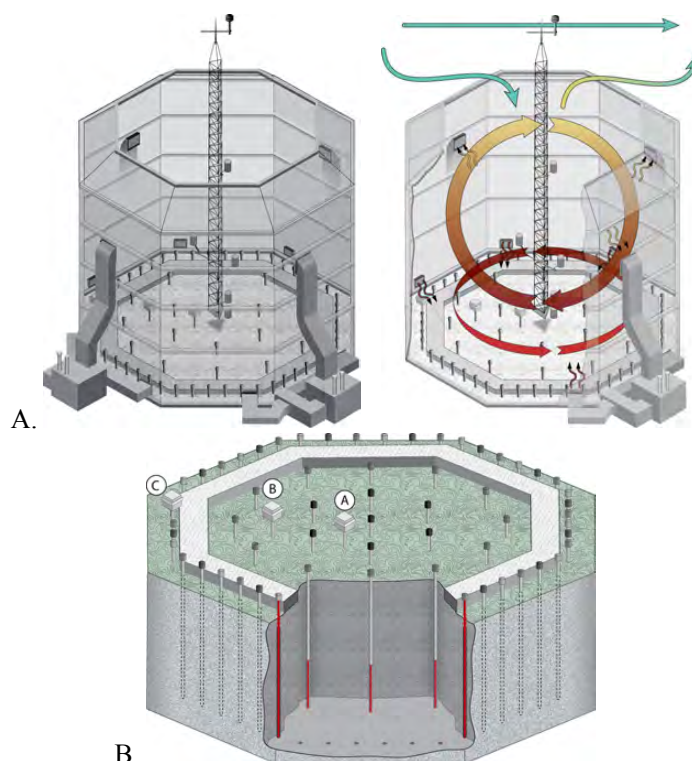
202 Air warming was achieved by heating the air above the surface of the peatland to a height of
203 nearly 6 m within open top octagonal enclosures (7 m tall by 12.8 m in diameter with an area of
204 114.8 m²; Fig. 2A). The enclosures include an octagonal open top (8.8 m diameter with an area
205 of 66.4 m²) bounded by a 35° frustum. The frustum was added to enhance the efficiency of the
206 warming enclosure (Barbier et al. 2012). Wall and frustum structural members were made of
207 structural aluminum (6061-T6 Alloy), and the walls are sheathed with double walled transparent
208 greenhouse panels (16 mm acrylic glazing). The vertical walls of the enclosure sit approximately
209 0.46 m above the bog hollow surface. The gap from the bottom of the enclosure was sealed into
210 the bog surface (~10 cm) with flexible acrylic panels. All structures are supported above the bog
211 on helical piles installed to a typical depth of 12 to 18 m below the peat surface within stable
212 ancient lake sediments and glacial till.

213

214



215



216

217 **Figure 2:** Panel A: Diagram of the air warming enclosure, warm air flow pattern, and external
218 wind inputs leading to a homogenized air envelope that surrounds the aboveground vegetation.
219 Panel B: Diagram of the belowground heater distribution pattern and the functional heating
220 surfaces. The 100 W heaters are deployed in an inner section A (7 deep only heaters), B (12 deep
221 only heaters), and C (three alternating circuits of 48 full length heaters).
222

223 Air warming method theory, protocols and optimization of an earlier prototype were fully
224 described by Barbier et al. (2012). Briefly, air at four mid-enclosure heights was drawn from
225 within the enclosure down to four ground level propane indirect fired bent tube heaters (Model
226 A2-IBT-600-300-300-G15; CaptiveAire, Youngsville, NC)) for variable heating of the air to
227 achieve five temperature targets (+0, +2.25, +4.5, +6.75 and +9 °C). The pattern of air flow and
228 air warming within a typical enclosure is depicted in Fig. 2A. Warmed air from the 4 heat
229 exchangers is split into eight equal distribution conduits for distribution into the enclosure 1
230 meter above the peat hollow surface through diffusers located on each wall. The control or warm
231 air delivered into each enclosure is provided at a continuous mean velocity of 7.5 m s^{-1} (blower
232 operation was initiated in 2015 as soon as each enclosure was fully glazed with greenhouse



233 panels). These warm air streams are directed away from adjacent vegetation surfaces as much as
234 possible and diffuse rapidly into the background mixed air of the enclosure.

235

236 The air warming described above was achieved using propane fired heat exchangers. Propane
237 was delivered to a large (10000 gallon) liquid propane storage tank located at the site. Liquid
238 propane was pulled from the bottom of this tank and pumped to vaporizers located at the head of
239 each boardwalk. Vaporized propane was then piped to the furnaces. This system allowed us to
240 operate throughout the year including periods of ambient winter temperatures as low as -35°C
241 on January 17, 2016.

242

243 **2.4 Peat warming protocols**

244 In June of 2014 when the capabilities for deep belowground warming were operational, we
245 initiated a 13-month period of DPH treatments for the 10 constructed SPRUCE plots. The DPH
246 method is an expanded form of the deep belowground heating approach of Hanson et al. (2011)
247 that was rationalized as being an appropriate surrogate for deep soil heating expected under
248 future climate conditions (Huang 2006; Baker et al. 1993). DPH was accomplished by an array
249 of 3-m vertical low wattage (100 W) heating elements installed throughout the plots within a
250 plastic-coated iron pipe. The belowground heating array, which was contained within the
251 encircling subsurface corral, included circles of 48, 12, and 6 heaters at 5.42, 4 and 2 m radii,
252 respectively (Fig. 2B). A single heater was also installed at the plot center. Exterior heaters in the
253 circle of 48 applied the 100 W across the full linear length of the heater, and all interior heaters
254 applied their 100 W heating capacity to the bottom one third of each resistance heater (pipe
255 thread core heaters, Indeco, St. Louis, MO). Interior heaters were different to avoid directly
256 heating the peat volumes targeted for the measurement of response variables.

257

258 **2.5 Temperature Control**

259 Simple proportional-integral-derivative (PID) control was used for aboveground heating based
260 on differentials measured by duplicate sensors in the center of the plot at +2 m. In the each above
261 ground heating system, the position of a liquid petroleum gas (LPG) valve in each of the four
262 heating units was simultaneously controlled. The belowground heating system controlled
263 individual heating circuits with silicon controlled rectifiers (SCR Controller: 1 Phase, 1 Leg.



264 240V, 20 Amb @42.5 °C; 4-20 mA control, Watlow Model DA10-24-F0-0-00) in each of 5
265 circuits. DPH within the experimental plots was achieved through PID control of three exterior
266 (the circle of 48 split into alternating thirds) and two interior circuits of the resistance heaters
267 shown in Fig. 2B. The control depth was -2 m. The reference for air and belowground heating
268 was the Plot 06 control plot. Details for above and belowground PID control are provided in the
269 supplemental materials to this paper along with PID coefficients for each warming treatment.

270

271 **2.6 Elevated CO₂ Additions**

272 Logical projections from IPCC analyses and the recent evaluation of current emissions (Raupach
273 et al. 2007; Collins et al. 2013) suggests that experimental methods might consider atmospheric
274 CO₂ concentrations at or above 800 ppm based on current fossil fuel use. As with the warming
275 targets, the goal of the SPRUCE infrastructure was not to simulate a specific future climate or
276 atmospheric condition, but to include a [CO₂] representative of the high end of predicted values
277 for the end of the century (Collins et al. 2013). The eCO₂ additions were included to better
278 understand the potential mechanism that CO₂-induced enhancements of gross primary production
279 might have on warming responses.

280

281 Pure CO₂ additions were initiated in half of the treatment plots (one for each temperature
282 manipulation) on 15 June 2016 to provide an eCO₂ atmosphere approaching 900 ppm (nominally
283 +500 ppm over current conditions in 2016) during daytime hours. The selected value is
284 purposefully higher than concentrations used in previous large eCO₂ experiments (Medlyn et al.
285 2015), and might be expected to yield a greater response by the trees and shrubs of the S1-Bog.
286 The following text briefly describes the mechanism for elevating CO₂ within the WEW
287 enclosures. Half-hourly assessments of [CO₂] in air were obtained at 0.5, 1, 2 and 4 m by
288 continuously sampling of air from plot-center tower locations via a sampling manifold.
289 Individual elevations were sampled in series for 90 seconds over a 6 minute cycle. The sampled
290 gas stream was analyzed using an in line LiCor LI-840 CO₂/H₂O gas analyzer at a flow rate of 1
291 L min⁻¹.

292

293 The presence of the enclosure walls reduces air turnover within the experimental space and limits
294 the amount of CO₂ needed as compared to Free-Air CO₂ Enrichment (FACE) studies (e.g.,



295 Dickson et al. 2000). Source CO₂ for the SPRUCE experiment was obtained from a fossil-fuel
296 based fertilizer plant by the contracted CO₂ supplier (Praxair, Inc.) and has $\delta^{13}\text{C}$ - and $\Delta^{14}\text{C}$ -CO₂
297 signatures of ~54 ‰ and -1000 ‰, respectively. Pure CO₂ from a central storage area (two 60-
298 ton refrigerated tanks) is vaporized and transferred by pipeline to each enclosure where it is
299 warmed and regulated before entering a mass flow control valve (model GFC77, 0-500 LPM
300 CO₂, 4-20 mA control; Aalborg Instruments and Controls, Inc.). The mass flow control valve
301 allows for variable additions of the pure CO₂ to the enclosure. A typical delivery velocity for
302 pure CO₂ equals 250 L min⁻¹, but ranges from 100 to 500 L min⁻¹ with external wind velocities
303 between 0.2 and 5 m s⁻¹ to account for increasing air volume turnover. Warm air buoyancy
304 increases with larger temperature differentials (Barbier et al. 2012) and increases air turnover
305 rates and demands for CO₂ additions.

306

307 The enclosure's regulated additions of pure CO₂ are distributed to a manifold that splits the gas
308 into four equal streams feeding each of the 4 air handling units (Fig. 2A), and is injected into the
309 ductwork of each furnace just ahead of each blower and heat exchanger. Horizontal and vertical
310 mixing within each enclosure homogenizes the air volume distributing the CO₂ along with the
311 heated air. Details of the CO₂ addition algorithms as they are impacted by external winds are
312 provided in the supplemental materials.

313

314 **2.7 Bog and Enclosure Environmental Measurements**

315 Half-hourly mean air temperature measurements were made with thermistors (Model HMP-155;
316 Vaisala, Inc.) installed at the center of each plot at 0.5, 1, 2 and 4 meters above the surface of the
317 peat. These same sensors included a capacitance sensor for the measurement of relative
318 humidity. New or recalibrated sensors are deployed annually or as comparisons to other sensors
319 suggest failure. Multipoint thermistor probes for automated mean half-hour peat temperature
320 measurements (W.H. Cooke & Co. Inc, Hanover, PA) were custom designed from a 1.3 cm
321 diameter x 0.9 mm wall stainless steel tube with a 7.62 cm stainless steel disk welded at the zero
322 height position along the tube. All elevations within the bog are referenced to the peat surface
323 hollows, which are defined to be an elevation of 0 cm. An electrical termination enclosure was
324 supported above the bog surface by a 46 cm extension of the measurement tube to avoid shading
325 the bog surface at the point of measurements and to keep it above any standing water. Peat



326 temperatures were recorded at 9 depths for the designated experimental plots (0, -5, -10, -20, -30,
327 -40, -50, -100 and -200 cm) at three concentric zones (one at 5.42-m radius; one at 3-m radius;
328 one at 1-m radius; Fig. 2B). All integrated temperature probes were located at a midpoint
329 between heaters in a given concentric ring of the plot. Hummock temperature measurements
330 were also obtained in the hummocks at various elevations above the hollow surface
331 (approximately 0, +10, and +20 cm).

332

333 Photosynthetically active radiation (PAR) was measured with quantum sensors (LiCor Inc., LI-
334 190R) at 2.5 m above the surface at a middle plot location. Supplemental 1-min short wave
335 (pyranometer, 300 to 2800 nm) and long wave (4.5 to 42 μm) radiation observations were also
336 measured using matched net radiometers (Model CNR4, Kipp and Zonen) for unchambered
337 ambient and within-enclosure locations for selected mid-summer days to further characterize the
338 enclosure environment.

339

340 Soil water content is difficult to measure in heterogeneous, low density organic soils.
341 Nevertheless, volumetric water content was measured within hummocks at two depths (0 cm at
342 the hollow surface, and 20 cm below hummock surface) at three locations within each plot using
343 a capacitance/frequency domain sensor (10HS, Decagon Devices Inc.). These sensors required
344 site-specific calibration (Supplemental Fig. S1).

345

346 External wind sensors at + 10 m above the center of each enclosure (Windsonic 4; Gill
347 Instruments) provided important information necessary to estimate the mixing of ambient air into
348 the enclosure space. A mobile 3-D sonic anemometer (Campbell Scientific Inc., Logan, Utah;
349 Model CSAT3B) was also temporarily deployed inside and outside of Plot 6 to characterize the
350 nature of turbulence changes inside and outside of the enclosures.

351

352 **2.8 Image collections**

353 Infrared imaging of the internal air space was done periodically to evaluate the spatial pattern of
354 heating of biological surfaces within the warming enclosures. Images were collected with a
355 thermal imaging camera (TiR4 #2816061, Fluke Corporation, Everett, WA) with a 20mm F/0.8
356 8-14 μm lens. Images were taken at the entrance of each enclosure (or unchambered ambient



357 space) immediately after the door was opened. All images in a comparative series were collected
358 before or after sunset within 20 minutes of one another (the time it takes to move about the
359 SPRUCE site).

360

361 Whole-plot visible wavelength image cameras (StarDot NetCam SC Series SD130BN 1.3MP
362 MJPEG Hybrid Color Day/Night IP Box Camera with 4mm Lens) were installed as a part of the
363 PHENOCAM network (Keenan et al. 2014; Toomey et al. 2015). These cameras provide a view
364 of the entire enclosure area. The whole plot imaging cameras record visible (400-700 nm) and
365 visible plus infrared (400-1000 nm) images sequentially, allowing calculation of NDVI-type
366 indices (Petach et al. 2014). They are installed on the southern wall of each enclosure at a height
367 of 6 m. Current and archived PHENOCAM images for the SPRUCE plots can be found at
368 <https://phenocam.sr.unh.edu/webcam/gallery/>.

369

370 **2.9 Energy Balance modeling**

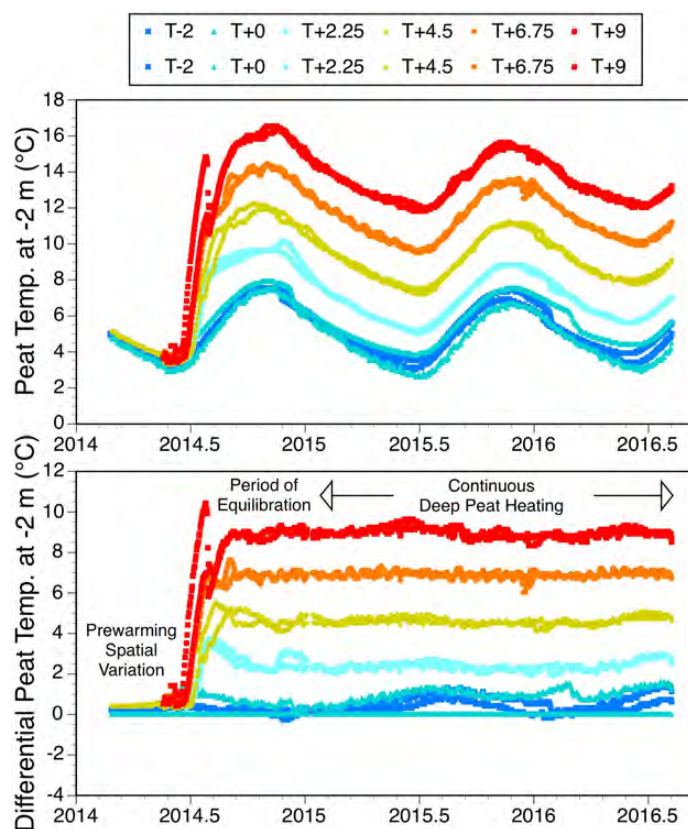
371 The energy balance in the S1 bog both inside and outside the enclosures was simulated using the
372 Community Land Model (CLM) version 4.5 (Oleson et al., 2013), which was modified to
373 represent the specific hummock-hollow microtopography, runoff and subsurface drainage at the
374 S1-Bog (Shi et al., 2015). This CLM-SPRUCE model was driven by meteorological data
375 collected by the environmental monitoring stations in the S1-Bog between 2011 and 2015.
376 Enclosure impacts on both incoming longwave and shortwave radiation were also considered in
377 the simulations. The incoming longwave radiation at the surface within an enclosure is estimated
378 by assuming the enclosure walls emit blackbody radiation at a temperature equal to the simulated
379 2-meter air temperature, and by using a sky view factor (defined as the proportion of the
380 longwave radiation received by the surface within the enclosure that comes from the clear sky)
381 of 0.3 to 0.35. The sky view factor is assumed to be 1 outside the enclosure (neglecting the
382 effects of the vegetation itself), while the inside values are calculated using the enclosure
383 geometry. The enclosure walls are also assumed to cause a 20% reduction in incoming
384 shortwave radiation. For these simulations, we do not consider the impacts of the enclosures on
385 wind speed, precipitation, or pressure. The effects of the enclosures on air and vegetation
386 temperature, snow cover, dew formation and energy fluxes are simulated by the model and
387 reported in the Discussion (Section 4).



388 3. Results

389 3.1 Warming Differentials

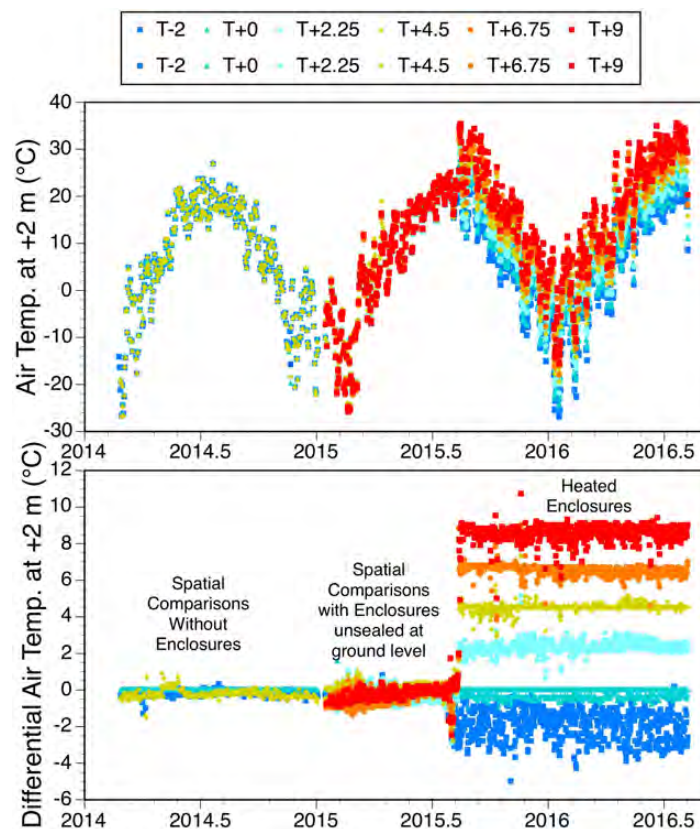
390 WEW in the S1-Bog was achieved by warming air throughout the vertical profile of tall
391 vegetation within an open topped enclosure combined with belowground warming using low-
392 wattage electrical resistance heaters optimized to the 12-m diameter space. Figure 3
393 demonstrates the effectiveness of the belowground heating method to produce a consistent deep
394 soil (peat) warming at -2 m beginning in the summer of 2014. Peat is also warmed below -2 m,
395



396 **Figure 3:** Daily mean deep peat temperatures (A) and the associated temperature differentials
397 (B) at -2 m by treatment plots since 2014 including the initial warm up periods (June through
398 early September 2014), and the sustained application of deep peat heating with air warming
399 (beginning September 2014). Differential temperatures are referenced to sensors within the fully
400 constructed but no-energy-added control Plot #6. Unchambered ambient plot data are also shown
401 as T-2 plots.
402
403



404 but continuous temperature monitoring below the -2 m zone was not done. Differential deep soil
405 temperature targets were sustained following periods of gradual heat accumulation from 22 to 94
406 days for the cooler and warmest treatments respectively (see Supplemental Table S3). Once deep
407 soil temperatures were achieved they were maintained consistently through time with the
408 exception of a few minor power interruptions or during instrument maintenance periods. Deep
409 soil temperatures in unchambered ambient plots (T-2 lines in Fig. 3) were warmer than the
410 designated reference control plot (Plot 6). Variation in the no-energy-added controls (Plot 6
411 versus Plot 19) represented spatial differences that were likely driven by variation in tree canopy
412 cover. Greater canopy cover (Plot 19) leading to warmer peat temperatures due to less heat loss
413 to the sky.



414
415 **Figure 4:** Daily mean air temperatures (A) and the associated air temperature differentials at +2
416 m above the bog surface by treatment plots since 2014 including periods prior to enclosure
417 construction (through January 2015), a period when upper enclosures were in place (January to
418 July 2015), and observations since full enclosure of each plot was achieved (27 July through 5
419 August 2015). Interior blower function was initiated at the time of full plot enclosure. The



420 sustained period of warming began at 14:00 on 12 August 2015. Differential temperatures are
421 referenced to sensors within the fully constructed but no-energy-added control Plot #6.
422 Unchambered ambient plot data are also shown as T-2 plots.
423

424 Figure 4 shows consistent pretreatment seasonal air temperature patterns across plots prior to the
425 full enclosure of the warming plots. Enclosure installations minus the bottom row of glazing was
426 completed between mid-January and early April of 2015. During the period from April through
427 July 2015 air handling units and duct work were installed. The bottom row of glazing was added
428 in mid-August 2015 followed immediately by the initiation of constant stirring of the internal air
429 space by the recirculating air handling furnaces. Air warming was initiated in all plots on August
430 12, 2015, and has been maintained near target levels since that time unless power outages or
431 system maintenance needs interrupted operation (Fig. 4).

432
433 Unchambered ambient plots are commonly from 1 to 3 °C cooler than the fully constructed
434 controls (Fig. 4), and plot to plot variation is responsible for the difference between our Plot 6
435 reference control and Plot 19 (the other no-energy-added control plot). The system based on PID
436 control of 2 m air temperatures at the center of each enclosure is routinely capable of maintaining
437 the differential temperatures for the +2.25 and +4.5 plots under virtually all environmental
438 conditions. Currently, at higher winds ($> 3 \text{ m s}^{-1}$) and for short periods of time the system
439 occasionally falls below the +6.75 and +9 °C target temperatures (especially in the +9 °C Plots
440 #10 and 17). We continue to work on adjustments to the PID settings to minimize such issues,
441 which are driven by the dilution of internal warm air by atypical cold air intrusions through the
442 enclosures open top.

443
444 Since the initiation of DPH on July 2, 2014 belowground warming has been actively engaged
445 greater than 98 % of the time for all plots except Plot 11 which was operated 93% of the time
446 (Table 1). Because the deep soils are largely self-insulated, downtime for active DPH
447 management resulted in only minor deviations from the target temperatures (Fig. 3). Active
448 aboveground warming, initiated on August 13, 2015, has been maintained greater than 99 % of
449 the time in 7 of 8 plots and more than 96.5 % of the time in Plot 11. When aboveground heating
450 fails for any reason, differential heating is lost almost immediately adding air temperature
451 variations greater than present in other plots that have not failed. Plot 11 downtime was the result



452 of Transect 2 power outages and winter issues with the air warming heat exchangers (i.e.,
 453 furnaces). Table 1 provides further details on the percent of days in which the mean temperature
 454 was within 0.2, 0.5, 1 or 1.5 °C of the established targets for a given treatment plot.

455

456 **Table 1.** Statistics for time of operation and time within operational target temperature ranges for
 457 each treatment enclosure or plot. (A) Percent of time for active deep peat heating (DPH) and
 458 whole ecosystem warming (WEW or air warming) since their respective inception in all
 459 treatment plots. (B) Percent of time belowground warming has been achieved since DPH targets
 460 were achieved in 2014. (C) Percent of time air warming has been achieved since August of 2015.
 461 NA = not applicable. All data are derived from daily mean air or soil temperature data.

462

Treatment Target Temperature	+0 °C*	+2.25 °C		+4.5 °C		+6.75 °C		+9 °C	
Plot #	19	11	20	4	13	8	16	10	17
A. Active Temperature Management									
DPH since 7/2/2014 (% days)	NA	93.0	98.3	98.3	98.3	99.7	98.1	96.6	98.3
WEW since 8/13/2015 (% days)	NA	96.5	99.6	100	99.6	99.1	100	100	100
B. DPH Statistics % Days within target °C									
Within 1.5 °C	100	100	100	100	100	100	100	100	100
Within 1.0 °C	67.4	100	100	100	100	100	100	100	100
Within 0.5 °C	22.8	93.2	100	99.6	100	100	98.5	92.2	100
Within 0.2 °C	1.0	80.3	79.6	54.1	98.7	89.6	64.5	54.9	56.3
C. WEW Statistics % Days within target °C									
Within 1.5 °C	99.5	95.6	99.5	98.7	97.4	91.7	98.7	93.9	95.2
Within 1.0 °C	99.5	93.8	97.8	98.2	95.2	84.6	96.9	78.5	72.4
Within 0.5 °C	51.3	91.2	85.1	89.5	71.9	57.0	67.5	46.1	37.3
Within 0.2 °C	4.4	73.7	47.4	49.6	36.8	21.9	33.8	21.9	17.1

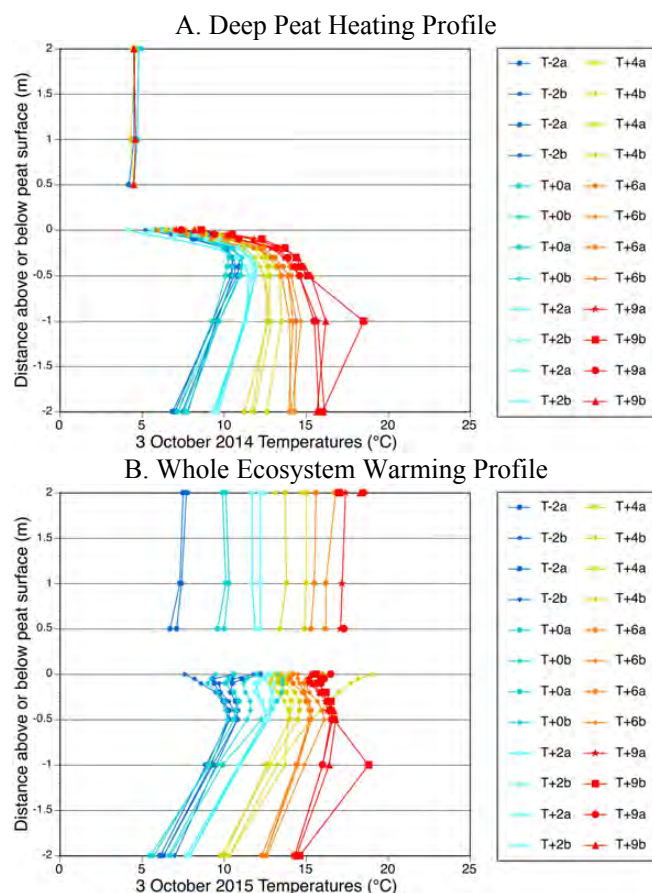
463 *Data for Plot #19 (the second constructed control plot with Plot 6 being the primary reference
 464 for this table) reflect spatial variation rather than heating system performance.

465



466 Detailed plot-by-plot measured temperature data for both below and aboveground heating are
467 available for viewing at the following web portal <http://sprucedata.ornl.gov>.

468
469



470
471

472
473

474 **Figure 5:** Temperature profiles from -2 m above through -2 m below the peat bog hollow surface
475 for (A) 3 October 2014 during deep peat heating, and (B) 3 October 2015 under whole
476 ecosystem warming. Air temperatures are the daily mean, and soil temperatures are the value
477 recorded at noon. Colors in the figure legend show data for unchambered ambient (T-2x), no-
478 energy-added control (T+0x) and warmed plots: +2.25(T+2x), +4.5(T+4x), +6.75(T+6x) and
479 +9(T+9x) °C, where x is either the a or the b series temperature zone within the plots.

480

481 3.2 Temperature profiles within the enclosures

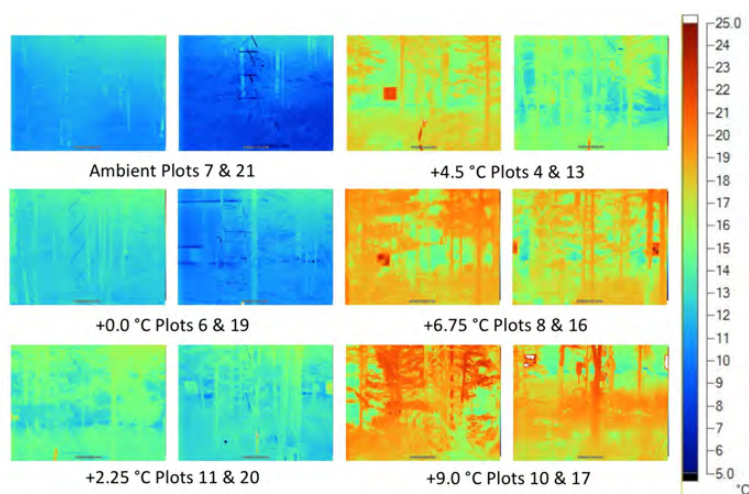
482 During the period of DPH, and continuing under WEW, DPH in the -1 to -2 m peat depth was
483 achieved (Fig. 3). During DPH, air temperatures were not different, and surface peat
484 temperatures did not achieve the full target warming temperatures due to heat losses to the



485 atmosphere (Fig. 5a). With the addition of air warming, target temperature differentials were
486 approximated from the tops of the enclosed trees to peat depths of at least -2 m (Fig. 5b). The
487 data in Fig. 5 are only single snapshots of these type of data, and some variation over time in the
488 near surface peat zone is expected due to rain and snow events that may temporarily upset local
489 energy balance. The divergence of one peat temperature pattern in the B-series for one of the
490 +4.5 °C temperature plots (Fig. 5B) resulted from proximal heating of that particular zone of soil
491 by a heated air sampling tubing bundle. The heated bundle has since been repositioned to
492 eliminate this local bias.

493

494 Horizontal air temperature patterns are minimal within the plots due to the stirring of the internal
495 air by the fans of the air heating system and the coupling with external air exchanges (Fig. 2A).
496 These phenomena are fully described in the description of the prototype enclosure published
497 previously (Barbier et al. 2012), but color infrared temperatures provide quantitative data in
498 support of the distribution of horizontal temperatures within the plots (Fig. 6 and supplemental
499 data Fig. S4).



500
501 **Figure 6:** Color infrared images for the space within the designated treatment enclosures taken
502 on September 10, 2015 after sunset within a 30-minute period. The thermal color scale in °C
503 applies to all images. Non-biological metal or plastic surfaces in the images may not provide an
504 accurate temperature due to their emissivity difference from biological surfaces.

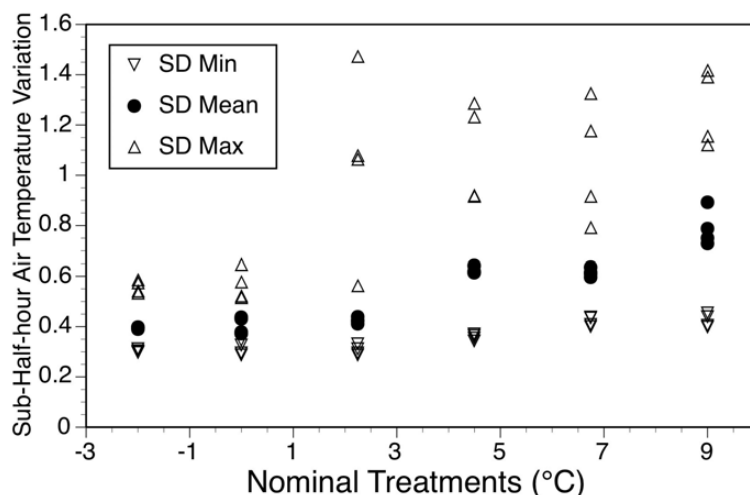
505
506
507



508 3.3 Temporal Temperature variation

509 It is useful to understand how both short (minute-by-minute) and longer-term (i.e., diurnal and
 510 seasonal) temporal variation within the enclosures compares between unchambered ambient and
 511 treatment plots. Figure 7 shows that control plots compare well to unchambered ambient
 512 conditions with almost no change in the standard deviation metrics for minute-by-minute
 513 observations within half hourly data. Conversely, the mean temperature standard deviations
 514 among one-minute data increase gradually with temperature treatments to nearly 2 times the
 515 nominal unchambered ambient standard deviation for the +9 °C treatment plots. Increased short-
 516 term variance results from temperature control inefficiencies.

517



518

519 **Figure 7:** Sub-half hour variation of air temperature data expressed as the standard deviation of
 520 1-min observations within a half hour measurement period. Plotted data are the daily minimum,
 521 mean and maximum half-hour temperature standard deviations over the period of observation for
 522 two replicate sensors in each treatment enclosure or plot. The -2 and 0 °C treatments in this
 523 graph represent unchambered ambient and no-energy-added control enclosures respectively.

524

525 Air temperature diurnal amplitudes for unchambered ambient plots ranged from 13.7 to 14.1 °C
 526 for warm season periods and 8.5 to 8.9 °C for cold season periods (Table 2). All treatment plot
 527 air temperature amplitudes remain within these diurnal ranges. Similarly, the unchambered
 528 ambient diurnal range for -2 m soil temperatures lies between 0 and 0.2 °C, which is matched in
 529 the treatment plots.

530

531



532 **Table 2.** Range of diurnal air temperature amplitudes (AT, °C) at + 2 m in warm (DOY 230 to
 533 300) and cold (DOY 300 to 365; 1 to 13) seasons, and the mean diurnal soil temperature
 534 amplitude (ST, °C) at – 2 m for a period including the warmest and coldest extremes of the
 535 measurement period (August 2015 – January 2016).

Treatment and Plots	Ambient Plots (7,21)	+0 °C Plots (6, 19)	+2.25 °C Plots (11, 20)	+4.5 °C Plots (4, 13)	+6.75 °C Plots (8, 16)	+9 °C Plots (10, 17)
Warm season AT diurnal amplitude	13.7 - 14.1	14.0 -14.1	13.0 - 13.7	13.3 - 13.5	13.9 - 14.2	13.2 - 13.6
Cold season AT diurnal amplitude	8.5 - 8.9	8.1 - 8.4	7.9 - 8.3	8.3 - 8.4	8.5 - 8.8	8.8 - 8.9
-2 m soil temperate diurnal amplitude	0.0 – 0.2	0.0 – 0.3	0.0	0.1 – 0.1	0.1 – 0.1	0.0 – 0.1

536 Annual amplitudes (approximated from summer maximums in 2015 and winter minimums in
 537 2016) for air temperatures (49 to 51 °C) and soil temperatures at – 2 m (DPH: 4 to 5 °C; WEW
 538 2.5 to 3.1 °C) are consistent among unchambered ambient and treatment plots (Table 3). The
 539 WEW system is capable of adding differential treatments to existing diurnal and seasonal
 540 temperature patterns.
 541

542 **Table 3.** Annual range of observed maximum minus minimum air temperature at + 2m (AT, °C)
 543 for the whole ecosystem warming (WEW) period from August 2015 through January 2016,
 544 which includes the warmest and coldest periods of an annual cycle. Also shown are the range of
 545 maximum minus minimum soil temperatures (ST) at -2 m throughout the deep peat heating
 546 period in 2014 and 2015, and the WEW period since August 2015.
 547

Treatment and Plots	Ambient Plots (7,21)	+0 °C Plots (6, 19)	+2.25 °C Plots (11, 20)	+4.5 °C Plots (4, 13)	+6.75 °C Plots (8, 16)	+9 °C Plots (10, 17)
+ 2 m AT for WEW	50.4 - 51.1	50.2 - 50.5	50.5	50.2 - 50.5	50.6 - 50.8	49.1 - 50.5
-2 m ST annual amplitude for DPH	4.0 – 4.4	4.0 – 4.9	4.5 – 5.1	4.9 – 4.9	4.9 – 5.0	4.6 – 4.9
-2 m ST annual amplitude for WEW	2.4 – 2.5	2.6 – 3.1	2.6 – 2.8	2.9 – 2.9	3.0 – 3.0	2.6 – 2.9

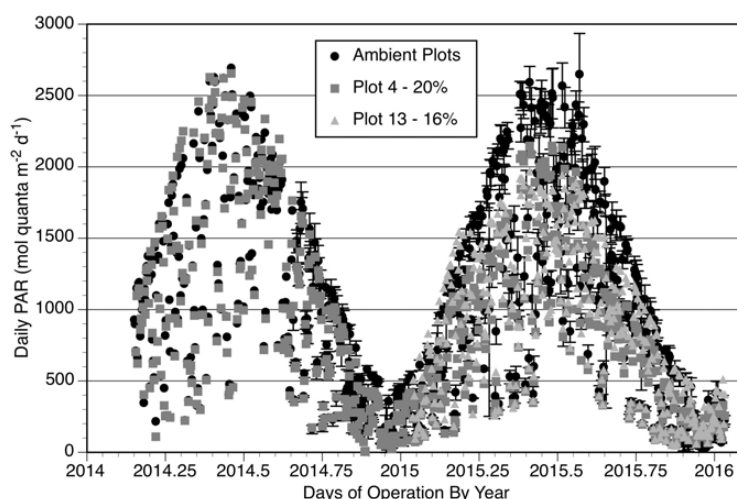
548
 549

550 3.4 Unchambered Ambient vs. Enclosure Environments

551 The mild belowground warming applied in SPRUCE produces minimal artifacts due to the deep
 552 soil target warming location and the low-wattage-heater application of energy. In contrast, the
 553 construction of walled enclosures to make air warming tenable produces a number of changes



554 from ambient conditions that need to be considered including: light, wind, humidity,
555 precipitation, dew formation, and snow and ice accumulation.
556



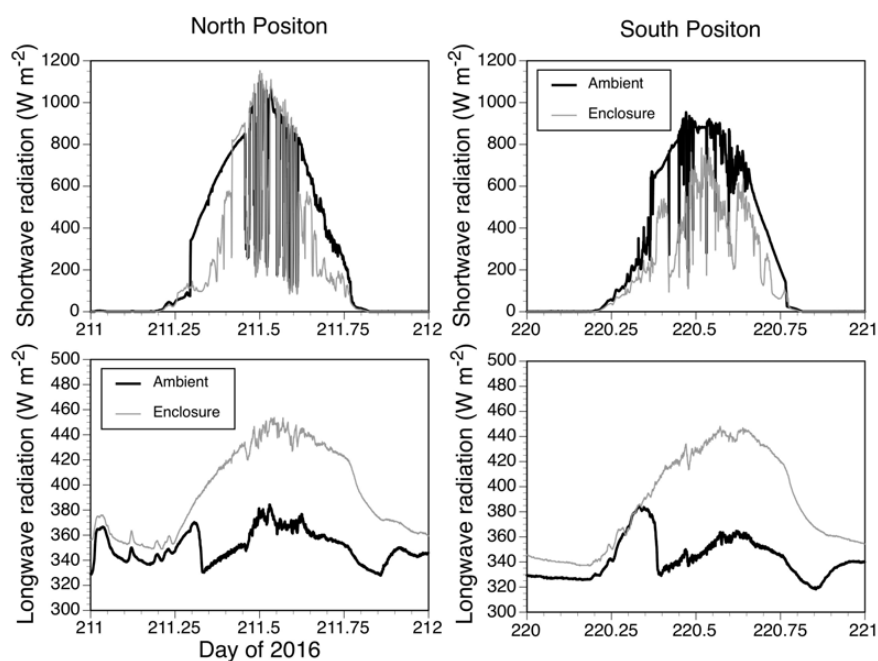
557
558 **Figure 8:** Example plot center daily photosynthetically active radiation (PAR) at 2.5 meters
559 above the bog surface in 2014 before enclosures were installed and after enclosure additions in
560 2015. The unchambered ambient plot data are from plot 7 (early in 2014) or the mean of plots 5,
561 7, and 21 with standard deviations shown. The figure legend shows the percent reduction in
562 annual cumulative PAR associated with the presence of the enclosure infrastructure.

563
564 Light levels within the plots before and after the installation of enclosures are plotted for selected
565 plots in Fig. 8. With the installation of the enclosure aluminum structure and the addition of
566 double-walled greenhouse glazing, midday PAR levels within the enclosures are reduced by
567 about 20 %. Under cloudy conditions or in the morning and evening when a greater fraction of
568 the light is diffuse, these differences are smaller. The greenhouse panels were not UV
569 transparent, but forest vegetation is known to largely tolerate UV light (Qi et al. 2010).

570
571 Short-wave and long-wave incident radiation data for the SPRUCE enclosures are reduced and
572 enhanced, respectively, when compared directly to matched data for unchambered ambient
573 conditions. Figure 9 shows examples of such data for a north and south centered location within
574 Plot 6 in the summer of 2016. When averaged over multiple mid-summer days the mean daily
575 reduction of incident short-wave radiation was 24.2 ± 2.4 % at north plot locations and 40.9 ± 3.7
576 % for fully impacted southern locations (i.e., area of the plot subjected to all frustum, glazing and
577 wall frame influences). Opposite the effect for short-wave radiation, increases in long-wave



578 radiation incident on the surface showed a mean daily increase of 10 ± 2 % increase, but
579 increases were greater in the daytime than for nighttime conditions (Fig. 9).
580

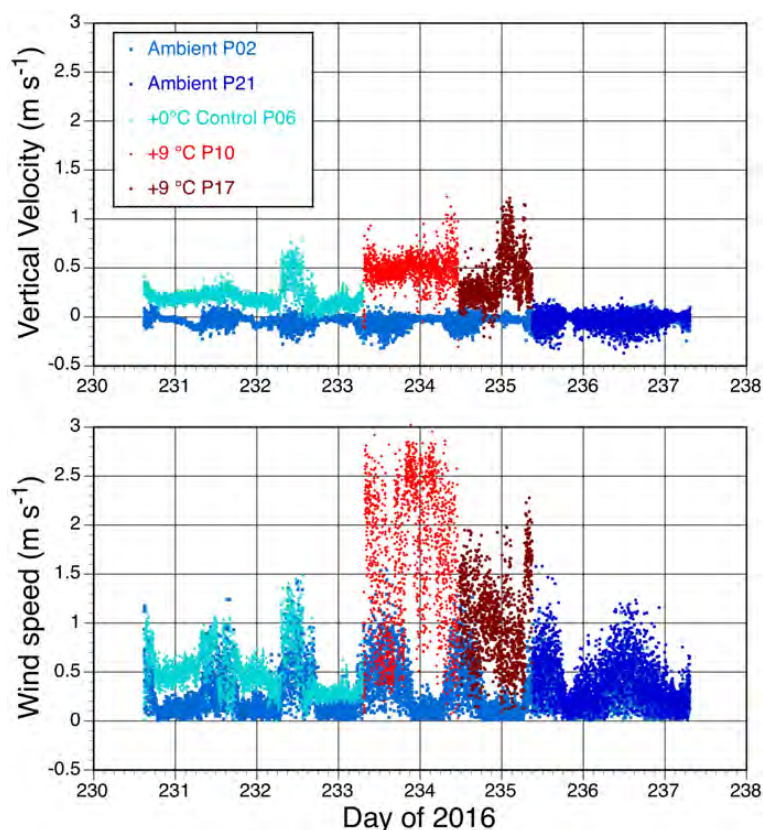


581
582 **Figure 9:** Example 1-minute incident short (upper graphs) and long-wave (lower graphs)
583 radiation data at north and south positions within the Plot 6 enclosure plotted against similar data
584 collected in unchambered ambient conditions. All data were collected approximately 2-m above
585 the surface of the S1-Bog boardwalks.
586

587 Ground level winds within the enclosures were necessarily enhanced to distribute heated air from
588 the edge sources to the center of the plot (Fig. 2A). To account for this enhanced wind effect, the
589 fully-constructed control applies the same air blowing system. While this provides a difference
590 between ambient conditions and treatment plots, it is fully controlled and comparable across all
591 heated enclosures. The air dynamics induced by external winds entering each enclosure through
592 the open top combined with internal turbulence generated by the blowers, homogenizes the air
593 volume inside the enclosure. Figure 10 shows a time series of vertical wind velocity and average
594 horizontal wind speed data contrasting unchambered ambient plots (Plots 2 and 21) with an
595 unheated enclosure (Plot 6) and the two +9 °C enclosures (Plots 10 and 17). There is more
596 turbulence in the enclosures than in ambient air and the turbulence increases with the level of
597 warming. Horizontal wind speeds are diurnally variable and comparable in both enclosed and



598 unchambered ambient plots. Vertical wind speeds are greater in the warming enclosures, increase
 599 with level of warming, and are always in the upwards direction both day and night.
 600



601
 602 **Figure 10:** One-minute vertical wind velocity (U_z ; upper graph) and mean horizontal wind
 603 speed (U_x and U_y ; lower graph) for unchambered ambient and enclosed plots of the SPRUCE
 604 study during the summer of 2016.

605
 606 Within the WEW enclosure total air turnover rates vary with external winds, and have been
 607 measured using the dilution of constant CO_2 additions. At external wind velocities less than 0.5
 608 m s^{-1} the enclosure air turns over approximately one time every 5 minutes. As winds approach 8
 609 m s^{-1} , the total air volume is turned over once per minute.

610
 611 Absolute humidity within the enclosures is conserved across treatments (Fig. S5). This is
 612 possible because of the wind induced turnover of air within the enclosures. Conversely, relative
 613 humidity (Table 4) varies by treatment. The environment within the fully constructed controls



614 closely matches ambient relative humidity, but relative humidity within the warmed plots drops
 615 proportionate to the warming treatments being only 51 to 55 % of the control for the most
 616 extreme warming treatment (+ 9°C; Table 4).

617

618 Although common in ambient settings, dew formation has not been observed in any of the
 619 warmed treatment enclosures, as relative humidity never reaches 100%. While this was to be
 620 expected for the warmed plots, we were not certain if dew would form in the no-energy-added
 621 control enclosures. In the control plots, RH does reach 100% on occasion, which would indicate
 622 some dew formation. Even so, the foliage in the control plots has not been visibly wet in the
 623 mornings, in stark contrast to the often heavy dew formation on foliage in unchambered ambient
 624 plots.

625

626 **Table 4.** Plot-to-plot variation in mean daily relative humidity \pm SD (RH; %) at +2 meters before
 627 the construction of enclosures (A), with enclosures (B), with active air warming treatments
 628 engaged during warm periods (C), and with heating during winter (D).

	Ambient Plots (7,21)	+0 °C Plots (6, 19)	+2.25 °C Plots (11, 20)	+4.5 °C Plots (4, 13)	+6.75 °C Plots (8, 16)	+9 °C Plots (10, 17)
A. Before*						
Max RH	99.0 \pm 0.2	98.8 \pm 0.0	NA	99.0 \pm 0.1	NA	NA
Mean RH	79.7 \pm 0.3	82.5 \pm 0.2	NA	79.3 \pm 0.1	NA	NA
Min RH	52.3 \pm 0.4	57.9 \pm 0.2	NA	52.6 \pm 0.0	NA	NA
B. With Enclosures**						
Max RH	99.6 \pm 0.1	99.7 \pm 0.1	99.2 \pm 0.3	99.7 \pm 0.1	99.5 \pm 0.2	99.4 \pm 0.4
Mean RH	77.4 \pm 0.7	77.9 \pm 0.6	76.9 \pm 0.3	77.6 \pm 0.5	77.1 \pm 0.6	76.8 \pm 0.7
Min RH	48.7 \pm 0.9	50.1 \pm 0.5	49.2 \pm 0.3	49.7 \pm 0.6	49.4 \pm 0.4	48.9 \pm 0.2
C. With Heating***						
Max RH	99.4 \pm 0.3	96.7 \pm 0.5	83.8 \pm 1.8	76.7 \pm 2.4	66.0 \pm 0.5	58.8 \pm 0.7
Mean RH	81.8 \pm 1.0	78.1 \pm 0.2	66.3 \pm 1.5	60.1 \pm 1.8	51.1 \pm 0.1	45.1 \pm 0.5
Min RH	54.5 \pm 0.9	51.9 \pm 0.1	44.7 \pm 1.0	40.6 \pm 1.2	33.7 \pm 0.5	30.4 \pm 0.6
D. Winter Heating****						
Max RH	95.7 \pm 0.4	92.6 \pm 0.7	77.6 \pm 1.0	68.6 \pm 1.4	59.6 \pm 1.2	53.0 \pm 1.6
Mean RH	89.2 \pm 0.6	85.7 \pm 0.4	70.2 \pm 0.9	61.1 \pm 1.1	53.0 \pm 0.9	46.8 \pm 2.9
Min RH	77.0 \pm 0.4	73.1 \pm 0.3	58.8 \pm 0.6	50.0 \pm 0.5	43.9 \pm 0.7	39.3 \pm 4.1

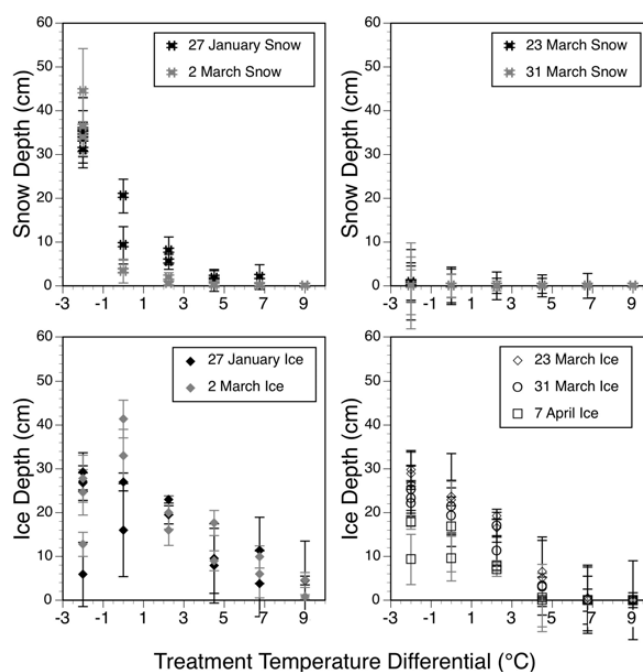
629 *Days compared = days of the year 160 to 200 in 2014. ** Days compared = days of the year
 630 160 to 200 in 2015; ***Days compared = days of the year 230 to 300 in 2015. ****Days
 631 compared = days of the year 335 in 2015 to 10 in 2016. NA = not available.



632

633 Apparent water content and rate of soil drying also varies across plots due to the heterogeneous
634 density of hollows and differential tree density. Even so, the rate of soil drying increased when
635 the plot heating began, and drying was positively correlated with increasing plot temperatures
636 indicating enhanced evapotranspirational demand (Jeff Warren, personal communication).

637



638

639 **Figure 11:** Snow depth (upper graphs) and ice depth (lower graphs) in each plot on January 27
640 and March 2, 23, 31 and April 7, 2016. All values are the mean depth \pm sd for 4 locations within
641 replicate plots represented by the target treatment temperature differentials.

642

643 3.5 Snow and Ice Accumulation

644 An area of uncertainty in the development of the WEW prototypes in eastern Tennessee (Barbier
645 et al. 2012) was how snow accumulation would develop within the plots when deployed in
646 Minnesota. Observations throughout the winter of 2015-2016 have shown that snow actively
647 accumulates within the enclosures with a more or less uniform distribution around the plots (Fig.
648 S6). Ground level blower effects are limited to the edges of the plots (data not shown). Active
649 snow enters all warmed treatment plots, but its accumulation as a snow layer depends on the
650 temperatures of the vegetation and peat surface. Snow has been seen to accumulate in all warmed
651 plots if overall conditions allow, but it thaws or sublimates much faster in the warmed plots. The



652 control enclosures did not accumulate as much snow as ambient locations, but ice accumulation
 653 within the peat profile can be equal to or greater than the accumulation in ambient areas at times
 654 (Fig. 11). During the spring of 2016 the warmed plots lost their snow cover and ice thawed faster
 655 than in the colder plots consistent with expectations for the experimental design.

656

657 3.6 Energy Use

658 The *in situ* WEW facility for tall statured plants was expensive to build yet cost-effective to
 659 operate given the nature of the treatments. Key daily energy requirements for each treatment plot
 660 under warm and cold season conditions are presented in Table 5. Soil warming using resistance

661

662 **Table 5.** Daily energy requirements for air and soil warming for the overall experiment and
 663 values for individual treatment plots.

Season	Warm Season Months (April to October)			Winter Months (November to March)		
	kW h d ⁻¹	Gallons LPG d ⁻¹	MJoules d ⁻¹	kW h d ⁻¹	Gallons LPG d ⁻¹	MJoules d ⁻¹
Air warming*						
Full Experiment	---	638	64,283	---	795	80,102
By Treatment**						
+0 °C Enclosure	---	0	0	---	0	0
+2.25 °C Enclosure	---	~31.9	~3,214	---	~39.7	~4,000
+4.5 °C Enclosure	---	~63.8	~6,428	---	~79.5	~8,010
+6.75 °C Enclosure	---	~95.7	~9,642	---	~119.25	~12,015
+9 °C Enclosure	---	~127.6	~12,857	---	~159	~16,020
Soil warming***						
Full Experiment	265	---	954	495	---	1,782
By Treatment						
+0 °C Enclosure	0	---	0	0	---	0
+2.25 °C Enclosure	9.0±1.7	---	32.4±6.1	12.6±0.8	---	45.4±3.0
+4.5 °C Enclosure	24.6±0.3	---	88.6±1.0	31.9±2.9	---	115.0±10.4
+6.75 °C Enclosure	38.8±7.1	---	139.7±25.5	46.7±11.0	---	168.3±39.5
+9 °C Enclosure	62.2±27.3	---	223.9±98.2	69.4±21.2	---	249.8±76.4
Blower Energy****	~2,222	---	7,999	~2,276	---	8,194

664 *1 Gallon liquid petroleum gas (LPG US) = 100.757 MJ. **Air warming requirements by
 665 treatment plots are only approximate and a derivation of total LPG use for the complete
 666 experiment. ***Soil warming is measured by treatment plot, but is compared to metered energy
 667 use by transect, which includes the energy for blowing air and the operation of instruments. 1
 668 kW h = 3.6 MJ. ****Derived from total energy use during whole ecosystem warming minus
 669 energy during deep peat heating for the respective periods.

670

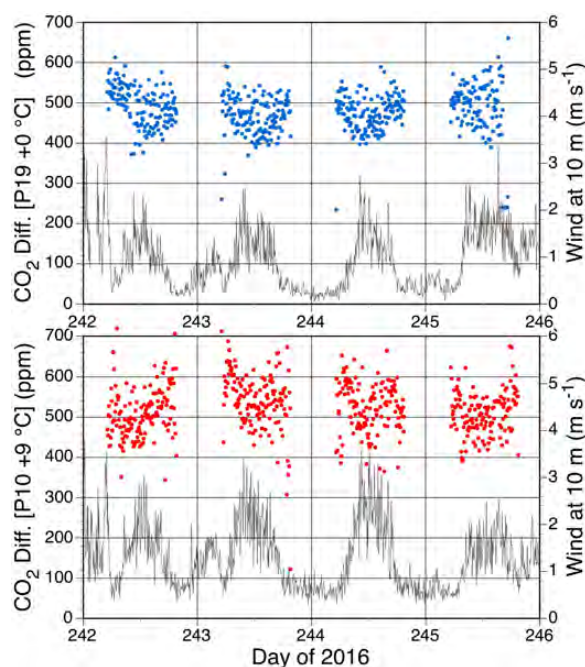


671 heating was continuously measured in amps converted to kW h. Air warming using liquid
 672 propane gas (LPG) for the full experimental site was estimated for each treatment in gallons of
 673 LPG. Both energy units were converted to MJoules to make direct comparisons among the
 674 warming methods. Air warming required 88 to 89% of the energy for WEW ranging from 64283
 675 MJ d⁻¹ during the warm season to 80102 MJ d⁻¹ during cold months. Soil warming required only
 676 1.3 to 1.9 % of the energy used ranging from 954 to 1782 MJ d⁻¹ of energy in the warm and cold
 677 seasons, respectively. Although not a direct energy requirement for warming, 9 to 11 % of the
 678 energy used was needed to drive the forced air blowers necessary to distributed warm air across
 679 the 12 m diameter enclosures.

680

681 3.7 Elevated CO₂ Treatments

682 The capacity for adding pure CO₂ of known isotopic signature (obtained from an ammonia
 683 production plant) to the air handling units of an enclosure to increase the atmospheric [CO₂] is
 684 demonstrated in Fig. 12. Based on 6-min running mean observations we have sustained a + 500
 685 ppm treatment within ±100 ppm using the current algorithms for a wide range of external wind
 686 speeds (Fig. 12).



687

688 **Figure 12:** Examples of the differential CO₂ concentrations achieved over 4 days in 2016 for a
 689 constructed control plot (+0 °C; upper graph) and plot warmed to +9 °C. All point data are 6-min



690 running mean [CO₂] differentials plotted with their respective 6-min running mean 10-m wind
691 speed data.

692
693 We are continuing to look at our control methods and will attempt to reduce the variation around
694 the target differentials. A comparison of these eCO₂ data with plot-to-plot variation for the non-
695 eCO₂ enclosures (Supplemental Table S5) suggests that the variation stems in part from spatial
696 variation hypothesized to be driven by localized differential air exchange between outside air and
697 the large enclosure volume. Warming and the buoyancy that it induces can also confound our
698 capacity to achieve a consistent +500 ppm eCO₂ treatment. The mean isotopic signature of the
699 elevated air was measured during the summer of 2016 as -22.6 ‰ δ¹³C and -517 to -564 ‰ Δ¹⁴C.

700

701 **4. Discussion**

702 Although there has been considerable discussion of the utility and merits of various warming
703 methods in recent years (Aronson and McNulty 2009; Amthor et al. 2010; Kimball 2011) we
704 chose to use air warming and deep soil warming for our studies, and have found the method
705 appropriate for warming a tall stature ecosystem (3 to 7 m) with active root and microbial
706 populations (> -2 m). The SPRUCE WEW enclosures provide us with the means to glimpse
707 warming futures at scales appropriate for the evaluation of peatland vegetation, microorganisms
708 and ecosystem functions. The SPRUCE enclosures are able to maintain the full range of
709 warming treatments (+2.25, +4.5, +6.75 and +9 °C) over external wind velocities ranging from 0
710 to as much as 6 m s⁻¹. The system allowed the application of the warming treatments largely
711 uninterrupted throughout a full annual cycle. The experimental systems were successfully
712 installed in a sensitive wetland ecosystem with minimal visible impact on the target plot
713 vegetation and underlying peat column. The warming treatments provide a reasonable
714 approximation of projected future climate and atmospheric boundary conditions within which to
715 study a full range of vegetation, microbial and biogeochemical cycling responses.

716

717 **4.1 Comparing WEW to other methods**

718 Other notable studies using either air warming or direct surface warming via infrared lamps have
719 also been deployed to understand warming responses for a range of ecosystems (Table 6;
720 Aronson and McNulty 2009, LeCain et al. 2015, Rustad et al. 2001). Air warming methods for



721 Table 6. Comparison of the SPRUCE WEW system characteristics to other representative plot scale warming approaches operated in
 722 field settings. Data are summarized at the individual plot level. Other warming studies not covered in this table of like studies are
 723 summarized by Rich et al. (2015), Aronson and McNulty (2009), LeCain et al. (2015) and Rustad et al. (2001).

Study/PI	SPRUCE WEW This Study	Black Spruce Plantation Bronson et al. 2008, 2009	B4Warmed Rich et al. 2015	PHACE LeCain et al. 2015	Peatland Bridgham et al. 1999	Temperate Seedlings Norby et al. 1997
Ecosystem	Picea-Sphagnum Bog	Picea mariana plantation	Deciduous forest Understory with planted seedlings	Northern mixed prairie	Bog and Fen Monoliths	Old Field Chambers
Lat. / Long. (degrees)	47.508 N -93.453 W	55.883 N -98.333 W	46.679 N; -92.520W & 47.946 N; -91.758 W	41.183 N; -104.900 W	47N; -92W	35.903 N; -84.339
Years of Operation	2015 to 2025	2004 - 2006	2009 - 2011	2006 – 2013 (detail 2010-2013)	1994	Various Studies 1994-2004
Differential treatments (+°C)	0*, 2.25, 4.5, 6.75, 9	0*, 5	0*, 1.8, 3.5	0*, 1.5 Day/3.0 Night	0*, 1.6-4.1	0*, 3
Heated plot Area (m²)	115.8	41.8	7.1	8.6	2.1	7.1
Use of a constructed control	Yes	Yes	Yes	Yes	NA	Yes
Season and Diurnal Operation	365 days, 24 hour	Heating treatments applied when control air > 0 °C	Warm season > 1 °C (208 to 244 days y ⁻¹); 24 hour	365 days, 24 hour	365 days, 24 hour	365 days, 24 hour
Aboveground Warming Method	Heated Air	Heated Air	Infrared Lamps	Infrared Lamps	NA	Heated/Cooled Air
Air T method and heights	Thermistors at 0.5, 1, 2(x2), and 4 m	Thermocouples at 1 and 2.5 m	IR Thermometer for the canopy surface	IR radiometers for the canopy/soil surface; Thermocouples at +25 cm, +15 cm (x2 within canopy)	NA	Thermistor 1 m
Volume of Heated Air surrounding vegetation (m³)	~911	~209	Not assessed	Not achieved	NA	17



Belowground Heating Method	Resistance heaters at 300 cm depth in an optimized pattern	Buried cables at -20 cm, 30 cm spacing	Buried cables at -10 cm, 20 cm spacing	NA	IR Surface Warming	Air Heating transfer
Soil T measurements and Depths (cm)	Thermistors at 0, -5, -10, -20, -30, -40, -50, -100, -200 at three locations in each plots	-2, -5, -10, -25, -50, -100	Type T thermocouples at -10 and a Subset at -20, -30, -50, -75, -100	-0.5 cm, -3 cm	Thermocouple at -15 cm	Thermistor -10 cm
Soil Temp Control Depth (cm)	-200	-20	-10	NA	NA	NA
Full Warming of soils below 1 m	Achieved	NA	Partial warming	NA	NA	NA
Volume of Fully Heated Soil (m³)	232	NA	~2.1	NA	NA	NA
eCO₂ Treatment	+500 $\mu\text{mol mol}^{-1}$	None	None	600 $\mu\text{mol mol}^{-1}$	None	+300 $\mu\text{mol mol}^{-1}$
eCO₂ Seasons of Operation	Growing season/daytime	NA	NA	Growing season, daytime	NA	Growing season, daytime
Other Details	Hydraulically isolated to 3 to 4 m using a sheet-pile corral	Irrigated, VPD control with mist addition	Trenched	Hydraulically isolated to -60 cm	Extracted Monoliths	Evaporative coolers
# Plots Operated	10	8	72	10	27	12
Design	Temperature Regression	2 heat x 2 irrigation, Randomized Complete Block	2 site x 2 habitat x 3 Temperature factorial	2 heat x 2 CO ₂ Factorial	2 peatland types (bog and fen) x 3 heat x 3 water table factorial	Various factorial designs

724 *A differential treatment of 0 implies the inclusion of fully constructed controls. NA = not applicable



725 field applications were established by Norby et al. (1997) for application to tree seedling and
726 Old-field research. They achieved air warming of +3 °C within 7.1 m² plots with limited soil
727 warming through air to soil heat transfer. Bronson et al. (2008, 2009) built larger air warming
728 chambers (41.8 m²) combined with soil warming cables to study an upland *Picea mariana*
729 plantation at +1.8 and +3.5 °C air warming and partial soil warming (i.e., near surface).

730

731 Infrared lamp warming studies have also been successfully used to study warming effects for
732 some time (Harte et al. 1995), and most recent field-scale infrared lamp studies have employed
733 designs based on Kimball et al. (2008). Notable for comparison to the SPRUCE peatland work
734 was the study by Bridgham et al. (1999) that used constant output infrared lamps to generate
735 seasonally realistic warming from +1.6 to + 4.1 °C in extracted peat monoliths. More recently
736 and for *in situ* work in prairie systems, LeCain et al. (2015) deployed infrared lamps over
737 hydraulically isolated plots achieving variable day/night canopy warming of +1.5/+3.0 °C,
738 respectively, and surface soil warming at 3 cm depth up to 3.8 °C. Rich et al. (2015) describe a
739 warming study targeting temperate seedling responses in an upland forest with a system using
740 infrared lamps and buried cables over trenched plots to warm vegetation canopy surfaces to +1.8
741 and +3.5 °C. They reported significant warming within the soil profile, but did not achieve full
742 deep soil warming consistent with their above ground temperature treatments. Notwithstanding
743 the lack of deep soil warming and unassessed air warming, the Rich et al. (2015) study is very
744 impressive encompassing two sites and a total of 72 treatment plots deployed in a factorial
745 design. Infrared heating designs for much larger plots than those used by these groups have also
746 been proposed (Kimball et al. 2011), and one such study is currently underway in a Puerto Rico
747 tropical forest understory using 4-m diameter plots (Tana Wood, personal communication;
748 Cavaleri et al. 2015). Where vegetation canopies are short in stature so as to receive reasonably
749 uniform heat from infrared lamps, the infrared method provides a viable field method for
750 gathering temperature response data for vegetation and surface soil organisms.

751

752 The Hanson et al. (2011) deep soil warming protocols modified for SPRUCE are also being
753 adopted in other recent ecosystem studies. Whole-soil and mesocosm warming experiments are
754 being conducted in mineral soil (Caitlin Hick Pries, personal communication), and a salt marsh
755 warming study using a modification of the deep soil heating approach has been initiated at the



756 Smithsonian Ecological Research Center in Maryland (Pat Megonigal, personal communication).
757 Another approach has been to focus on single tree enclosures, as demonstrated by Medhurst et al.
758 (2006) who used fully-enclosed, aboveground whole-tree air warming of individual *Picea abies*
759 trees (8.3 m² plots) maintained air at +2.8 to +5.6 °C, and included eCO₂ control. That system
760 has subsequently been deployed for *Eucalyptus* studies in Australia (Barton et al. 2010). The
761 Medhurst approach was not fully integrated with belowground warming and associated
762 processes, but it did allow continuous assessments of the carbon exchange of the enclosed
763 vegetation. Whole-enclosure carbon exchange calculations are planned for the SPRUCE study
764 using a modified eddy flux constrained assessment for ambient-CO₂ enclosures (Lianhong Gu,
765 personal communication).

766

767 Less technologically intense passive studies of warming, not covered in the reviews mentioned
768 earlier, include a peat monolith transplant study down an elevation gradient allowing the
769 characterization of a +5 °C temperature change (Bragazza et al. in press), a snow depth
770 manipulation deployed in the arctic (Natali et al. 2011), and evaluations of thermal gradients
771 around a geothermal source in Iceland (O’Gorman et al. 2015). While differing in plot sizes,
772 level of above and belowground temperature control or assessment, and the ability to standardize
773 methods, these approaches represent alternate methods from which to gather information on
774 vegetation and microbial system responses to warming.

775

776 **4.2 Unique Characteristics of the WEW Method**

777 The following text describes and discusses the influence of the WEW enclosures and treatments
778 on environmental variables that were altered from expected ambient conditions including: light,
779 wind, humidity, precipitation, ice and dew formation.

780

781 **4.2.1 Light**

782 The presence of greenhouse glazing and the enclosure structure reduced incident PAR at the
783 center of the enclosures by around 20% during midday periods. This level of reduction is not
784 sufficient to limit the photosynthetic capacity of the *Picea* foliage (Jensen et al. 2015) nor the
785 other photosynthetic forms of vegetation being studied (Jeff Warren, personal communication).
786 Reductions in short-wave radiation ranged from 24 to 41% and varied within the enclosure along



787 a south to north gradient. Long-wave or far infrared radiation representative of sky/cloud
788 temperature conditions were 10% greater than for ambient conditions leading to less heat loss at
789 night in constructed chambers when compared to unchambered ambient plots.

790

791 **4.2.2 Wind**

792 The increase in enclosure turbulence in warming and control plots is driven by forced air
793 movement from the hot air blower system, and confounded by the influence of vertical warm air
794 buoyancy. Increased horizontal turbulence is present in the unheated control enclosures
795 (0.14 ± 0.24 to 0.31 ± 0.23 m s⁻¹), and much larger in the +9 °C heated chambers (0.8 ± 0.4 to
796 1.3 ± 0.9 m s⁻¹). Vertical velocities (U_z) in the control and +9°C plots, show increases of
797 0.26 ± 0.18 m s⁻¹ for the Plot 6 control, and for the ±9 °C treatment enclosures 0.55 ± 0.14 m s⁻¹ for
798 Plot 10 and 0.41 ± 0.24 m s⁻¹ for Plot 17. A more detailed analysis of turbulence patterns across
799 the full range of warming enclosures will be evaluated in the future with planned deployment of
800 eddy flux instrument packages within the ambient-CO₂ enclosures for whole-enclosure-footprint
801 CO₂ and CH₄ flux measurements.

802

803 **4.2.3 Atmospheric humidity**

804 Warming of the enclosure using air containing consistent absolute humidity (supplemental data
805 Fig. S5) led to proportionate reductions in relative humidity (Table 4) and sustained a higher
806 gradient of vapor pressure between the well mixed enclosure air and wetter soil and plant
807 surfaces. Although not to the levels induced by the SPRUCE treatments, the most recent IPCC
808 report (Collins et al. 2013) concluded that relative humidity over interior continental regions
809 could be projected to drop with future warming. Some prior warming studies have considered
810 how to ameliorate this drop in humidity and reduction in soil water use by use of a steam/misting
811 system or irrigation in warmed plots (e.g., Bronson et al. 2008, 2009; De Boeck (2012)

812

813 Steam addition to sustain relative humidity within small open-topped warming chambers has
814 been shown to be technologically feasible (Hanson et al. 2011), however, it was not considered
815 for deployment at SPRUCE due to the requisite energy costs and water volume requirements.
816 For example, let us assume a mid-summer condition (25 °C, 97 kPa, 90-100 % day/night RH)
817 and continuous operation of our 911 m³ open top enclosures at + 9 °C with a mean external wind



818 velocity of 2 m s^{-1} , an enclosure turnover fraction of approximately 0.62 (actually external winds
819 and turnover fractions are often much greater), and a day/night RH of 47/70 %. Under these
820 conditions, a water source of $9.7 \text{ m}^3 \text{ d}^{-1}$ would have been needed for routine operations along
821 with additional energy to convert it to steam would have been required to sustain the ambient
822 relative humidity of 90% within the $+9 \text{ }^\circ\text{C}$ enclosure. Such a distilled water supply (necessary to
823 limit corrosion and nutrient transfers to the ecosystem) and energy supplies made RH control too
824 expensive. A mist based approach for controlling humidity in a free air environment has been
825 reported (Kupper et al. 2011), but such a system still requires the availability of a significant
826 treated water source and would increase the air warming heating demands necessary to sustain
827 our air warming differential temperatures due to the latent heat absorbed by evaporating droplets.
828

829 Choosing to operate our WEW system with variable relative humidity led to greater proportional
830 surface evaporation from *Sphagnum* (essentially all ground cover), water use by C3 plants and an
831 expected reduction in the seasonal water table with warming. In the first season of operation,
832 reductions in water table depths were limited as the corralled plots were left undrained and
833 ambient rainfall inputs exceeded losses from evapotranspiration. Since relative humidity was
834 allowed to vary with treatments in SPRUCE, significant effort was invested in fully quantifying
835 the impact on changing surface sphagnum and peat water content, plot level water balance, and
836 water table depth within each enclosure.

837

838 **4.2.4 Precipitation and Winter Ice**

839 Although the frustum encircling the top of the enclosure does create an internal rain and snow
840 shadow over the internal boardwalk, the excluded rain runs down the enclosure walls onto the
841 peat surface inside of the corral barrier. As a result, there is a rain shadow impact for some edge
842 vegetation, but the overall water inputs to the plot remain the same as for an unchambered
843 ambient plot (data not shown). The frustum does, however, reduce winter snow accumulation
844 within the plot because some snow is thrown clear of the subsurface corral (Fig. 11). However,
845 ice formation in the surface peat of the control plots was similar to or greater than that found
846 beneath unchambered ambient plots (Fig. 11).

847



848 Changes to the energy balance due to the presence of the enclosure (described above) have a
849 large impact on snow depth between unchambered ambient and enclosed plots. Simulations with
850 the CLM-SPRUCE model indicate that on average, the snow depth is reduced by 40% in
851 enclosed vs. unchambered ambient plots, with the highest reductions in the late winter and early
852 spring. Complete loss of snowpack generally occurs 2-3 weeks earlier when the effects of the
853 enclosure are considered. The observed reductions are slightly larger, reflecting enclosure snow
854 shadowing effects and potentially higher sublimation caused by increased air movement not
855 considered in the simulations. Despite the reduction in snow cover, the simulated ice depth is
856 similar between the unchambered ambient and enclosed plots – and this correlates well with our
857 *in situ* observations (Fig. 11). The warming of the peat layers caused by increased longwave
858 input is likely compensated to a large degree by increased heat loss during cold snaps because of
859 the reduction of insulating snowpack, an effect that was explained in more detail in Shi et al.
860 (2015).

861

862 **4.2.5 Lack of dew formation**

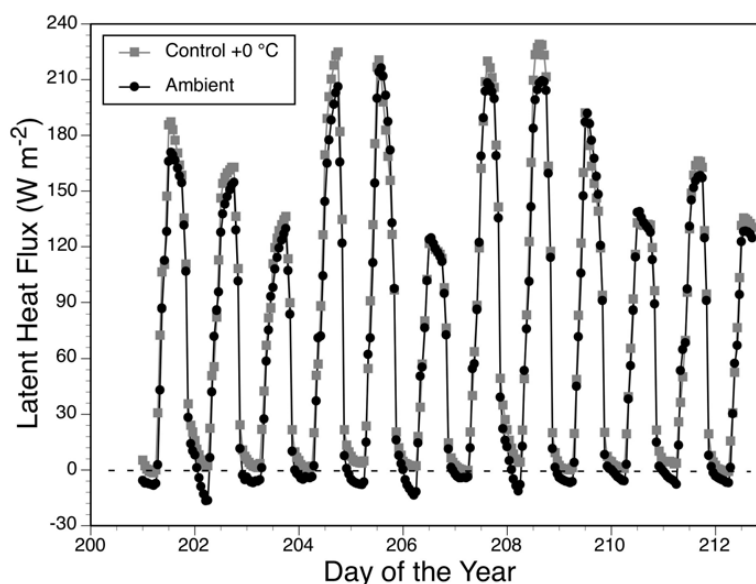
863 Even without active warming, modifications to the energy balance caused by the enclosures lead
864 to warming effects that influence air and vegetation temperatures, dew formation and snow
865 dynamics. The incoming longwave radiation within the enclosure is significantly elevated,
866 especially in clear-sky conditions. Simulations with the CLM-SPRUCE model (Shi et al., 2015)
867 were conducted to investigate the effects of SPRUCE enclosures on changes in the energy
868 balance on dew formation, snowpack and soil ice. Simulated average 2m air temperatures within
869 the enclosures are about 0.8 °C warmer than the unchambered ambient plots. This warming
870 effect is highly variable, ranging from nearly zero to over 5°C, and is largest in the early morning
871 under clear conditions, when radiation cooling is inhibited most by the enclosure walls, and
872 during the winter months when longwave radiation is a larger fraction of the overall radiation
873 budget. While the observed differences follow this general pattern, they are more than double the
874 simulated magnitudes. This may be due to the model ignoring the impacts of the enclosure on
875 wind speed and turbulence patterns, which cannot be considered in these simulations because the
876 assumptions in CLM-SPRUCE about Monin-Obukhov similarity and logarithmic wind profiles
877 (Oleson et al., 2013) that cannot easily be extended to the SPRUCE conditions. Simulated leaf



878 surface temperatures in the enclosures were elevated on average by 2.5°C, which has important
879 implications for carbon and energy fluxes.

880

881 Despite the underestimate of air warming in the simulation, the model results indicated a near
882 complete inhibition of dew formation (Fig. 13), similar to site observations. Total dew



883

884 **Figure 13:** Simulations of latent heat flux over a 10-day period for ambient conditions (black)
885 and in a control enclosure (grey) using environmental driver meteorology data from July 2013.
886 Negative latent heat fluxes indicate dew formation, but only occur for the ambient condition.

887

888 formation was about 12mm integrated over the growing season (May-September) in the ambient
889 simulation, but only 0.5mm in the enclosure simulation (96% reduction). In the simulations, this
890 resulted from higher surface temperatures and lower relative humidity. Near-surface wind speeds
891 in the enclosures are also usually higher than for unchambered ambient areas as a result of the
892 blowers. This turbulence likely further inhibits the formation of dew, but such an effect was not
893 considered in the CLM simulations.

894

895 5. Conclusion

896 The WEW system described is capable of providing a broad range of warming conditions up to +
897 9 °C with minimal artifacts from the experimental infrastructure. The end result is an experiment
898 system capable of giving scientists a fair glimpse of organism and ecosystem responses for



899 plausible future warming scenarios that can't be measured today or extracted from the historical
900 record. The large SPRUCE enclosures allow ongoing ecosystem-level assessments of warming
901 responses for vegetation growth and mortality, phenology changes, changing microbial
902 community composition and function, biogeochemical cycles and associated net greenhouse gas
903 emissions.

904

905 **6. Data Availability**

906 The environmental measurement data referenced in this paper are archived at and available from,
907 the SPRUCE long-term repository (Hanson et al. 2016; <http://mnspruce.ornl.gov>).

908

909 **7. Author Contributions**

910 P. Hanson conceived the experimental methods and wrote this paper. C. Barbier optimized the
911 air warming system using complex fluid dynamics models. J. Riggs programmed the SPRUCE
912 enclosure feedback control systems. M. Krassovski designed and maintained the local and
913 satellite communications systems. P. Hanson, W.R. Nettles, J. Phillips, J. Riggs and J. Warren
914 installed and maintain instrumentation. A. Richardson supplied installed and monitored plot
915 phenology cameras. D. Aubrecht evaluated light transmission characteristics of the enclosure
916 sheathing. L. Gu interpreted wind velocity and speed data. D. Ricciuto executed runs of the
917 CLM-SPRUCE model to interpret enclosure energy balance properties. LA Hook archived data.
918 All authors have read, understand and agree to the content of this paper.

919

920 **8. Acknowledgments**

921 The authors would like to thank Dr. Randall K. Kolka, USDA Forest Service for working in
922 collaboration with the Oak Ridge National Laboratory to enable access to and use of the S1-Bog
923 of the Marcell Experimental Forest for the SPRUCE experiment and affiliated studies. We would
924 also like to thank Natalie A. Griffiths, Stan D. Wullschleger and Randall K. Kolka for their
925 comments on early drafts, as well as editorial assistance provided by Terry Pfeiffer.

926

927 This material is based upon work supported by the U.S. Department of Energy, Office of
928 Science, Office of Biological and Environmental Research. Oak Ridge National Laboratory is
929 managed by UT-Battelle, LLC, for the U.S. Department of Energy under contract DE-AC05-



930 00OR22725. The development of PhenoCam IT infrastructure was supported by NSF's
931 Macrosystems Biology program (award EF-1065029).
932



933 **9. References**

934 Amthor, J.S., Hanson, P.J., Norby, R.J., Wullschleger, S.D.: A comment on “Appropriate
935 experimental ecosystem warming methods by ecosystem, objective, and practicality” by Aronson
936 and McNulty”, *Agric. For. Meteor.*, 150, 497-498, 2010.

937

938 Aronson, E.L., McNulty, S.G.: Appropriate experimental ecosystem warming methods by
939 ecosystem, objective and practicality, *Agric. For. Meteor.*, 149, 1791-1799, 2009.

940

941 Baker, D.G., Ruschy, D.L.: The recent warming in eastern Minnesota shown by ground
942 temperatures. *Geophys. Res. Let.*, 20, 371-374, DOI: 10.1029/92GL02724, 1993.

943

944 Barbier, C., Hanson, P.J., Todd, D.E. Jr., Belcher, D., Jekabson, E.W., Thomas, W.K., Riggs,
945 J.S.: *Air Flow and Heat Transfer in a Temperature Controlled Open Top Enclosure*, ASME
946 International Mechanical Engineering Congress and Exposition, 2012, Houston, TX, Paper
947 #IMECE2012-86352, 2012.

948

949 Barton, C.V.M., Ellsworth, D.S., Medlyn, B.E., Duursma, R.A., Tissue, D.T., Adams, M.A.,
950 Eamus, D., Conroy, J.P., McMurtrie, R.E., Parsbyg, J., Linder, S.: Whole-tree chambers for
951 elevated atmospheric co2 experimentation and tree scale flux measurements in south-eastern
952 Australia: The Hawkesbury forest experiment. *Agric. For. Meteor.*, 150, 941-951, 2010.

953

954 Bragazza, L., Buttler, A., Robroek, B.J.M., Albrecht, R., Zaccone, C., Jassey, V.E.J.: Persistent
955 high temperature and low precipitation reduce peat carbon accumulation, *Global Change Biol.*,
956 22, 3253-3254. doi:10.1111/gcb.13319, 2016.

957

958 Bridgham, S.D., Pastor, J., Updegraf, K., Malterer, T.J., Johnson, K., Harth, C., Chen, J.:
959 Ecosystem control over temperature and energy flux in northern peatlands. *Ecol. App.*, 9, 1345-
960 1358, 1999.

961

962 Bridgham, S.D., Megonigal, J.P., Keller, J.K., Bliss, N.B., Trettin, C.: The carbon balance of
963 North American wetlands, *Wetlands*, 26, 889-916, 2006.



964

965 Bronson, D.R., Gower, S.T., Tanner, M., Van Herk, I.: Effect of ecosystem warming on boreal
966 black spruce bud burst and shoot growth, *Global Change Biol.*, 15, 1534-1543, 2009.

967

968 Bronson, D.R., Gower, S.T., Tanner, M., Linder, S., Van Herk, I.: Response of soil surface CO₂
969 flux in a boreal forest to ecosystem warming, *Global Change Biol.*, 14, 856-867, 2008.

970

971 Cavaleri, M.A., Reed, S.C., Smith, W.K., Wood, T.E.: Urgent need for warming experiments in
972 tropical forests, *Global Change Biol.*, 21, 2111–2121. doi:10.1111/gcb.12860, 2015.

973

974 Collins, M., Knutti, R., Arblaster, J., Dufresne, J-L., Fichet, T., Friedlingstein, P., Gao, X.,
975 Gutowski, W.J., Johns, T., Krinner, G., Shongwe, M., Tebaldi, C., Weaver, A.J., Wehner, M.:
976 Long-term Climate Change: Projections, Commitments and Irreversibility. In: *Climate Change*
977 *2013: The Physical Science Basis. Contribution of Working Group I to the Fifth Assessment*
978 *Report of the Intergovernmental Panel on Climate Change* [Stocker, T.F., D. Qin, G.-K. Plattner,
979 M. Tignor, S.K. Allen, J. Boschung, A. Nauels, Y. Xia, V. Bex and P.M. Midgley (eds.)].
980 Cambridge University Press, Cambridge, United Kingdom and New York, NY, USA, 2013.

981

982 Cottingham, K.L., Lennon, J.T., Brown, B.L.: Knowing when to draw the line: designing more
983 informative ecological experiments, *Front. Ecol. Environ.*, 3, 145-152, 2005.

984

985 Cramer, W., Bondeau, A., Woodward, F.I., Prentice, I.C., Betts, R.A., Brovkin, V., Cox, P.M.,
986 Fisher, V., Foley, J.A., Friend, A.D., Kucharik, C., Lomas, M.R., Ramankutty, N., Sitch, S.,
987 Smith, B., White, A., Young-Molling, C.: Global response of terrestrial ecosystem structure and
988 function to CO₂ and climate change: results from six dynamic global vegetation models, *Global*
989 *Change Biol.*, 7, 357-373, 2001.

990

991 Davidson, E.A., Janssens, I.A.: Temperature sensitivity of soil carbon decomposition and
992 feedbacks to climate change, *Nature*, 440, 165-173, 2008.

993



- 994 de Boeck, H.J., Kimball, B.A., Miglietta, F., Nijs, I.: Quantification of excess water loss in plant
995 canopies warmed with infrared heating, *Global Change Biol.*, 18, 2860-2868, 2012.
996
- 997 Dickson, R.E., Lewin, K.F., Isebrands, J.G., Coleman, M.D., Heilman, W.E., Riemenschneider,
998 D.E., Sober, J., Host, G.E., Zak, D.R., Hendrey, G.R., Pregitzer, K.S., Karnosky, D.F.: *Forest*
999 *atmosphere carbon transfer and storage (FACTS-II) the aspen Free-air CO₂ and O₃ Enrichment*
1000 *(FACE) project: an overview*, Gen Tech. Rep. NC-214. St. Paul, MN: U.S. Department of
1001 Agriculture, Forest Service, North Central Research Station. 68 p, 2000.
1002
- 1003 Hanson, P.J. and others: *Ecosystem Experiments: Understanding Climate Change Impacts On*
1004 *Ecosystems and Feedbacks to the Physical Climate*. Workshop Report on Exploring Science
1005 Needs for the Next Generation of Climate Change and Elevated CO₂ Experiments in Terrestrial
1006 Ecosystems. 14 to 18 April 2008, Arlington, Virginia,
1007 http://science.energy.gov/~media/ber/pdf/Ecosystem_experiments.pdf, 2008.
1008
- 1009 Hanson, P.J., Childs, K.W., Wullschleger, S.D., Riggs, J.S., Thomas, W.K., Todd, D.E., Warren,
1010 J.M.: A method for experimental heating of intact soil profiles for application to climate change
1011 experiments, *Global Change Biol.*, 17, 1083–1096, 2011.
1012
- 1013 Hanson, P.J., Riggs, J.S., Nettles, W.R., Krassovski, M.B., Hook, L.A.: *SPRUCE Whole*
1014 *Ecosystems Warming (WEW) Environmental Data Beginning August 2015*. Carbon Dioxide
1015 Information Analysis Center, Oak Ridge National Laboratory, U.S. Department of Energy, Oak
1016 Ridge, Tennessee, U.S.A. <http://dx.doi.org/10.3334/CDIAC/spruce.032>, 2016.
1017
- 1018 Harte, J., Torn, M.S., Chang, F-R., Feifarek, B., Kinzig, A.P., Shaw, R., Shen, K.: Global
1019 warming and soil microclimate: results from a meadow-warming experiment. *Ecol. Appl.*, 5,
1020 132-150, 1995.
1021
- 1022 Huang, S.: Land warming as part of global warming, *EOS*, 87, 477, 480. 2006.
1023



- 1024 IPCC 2014: Climate Change 2014: Impacts, Adaptation, and Vulnerability. Part B: Regional
1025 Aspects. Contribution of Working Group II to the Fifth Assessment Report of the
1026 Intergovernmental Panel on Climate Change [Barros, V.R., C.B. Field, D.J. Dokken, M.D.
1027 Mastrandrea, K.J. Mach, T.E. Bilir, M. Chatterjee, K.L. Ebi, Y.O. Estrada, R.C. Genova, B.
1028 Girma, E.S. Kissel, A.N. Levy, S. MacCracken, P.R. Mastrandrea, and L.L. White (eds.)].
1029 Cambridge University Press, Cambridge, United Kingdom and New York, NY, USA, pp. 688,
1030 2014.
- 1031
- 1032 Kardol, P., De Long, J.R., Sundqvist, M.K.: Crossing the threshold: the power of multi-level
1033 experiments in identifying global change responses, *New Phytol* 196, 323-326, 2012.
- 1034
- 1035 Kayler, Z.E., De Boeck, H.J., Fatichi, S., Grünzweig, J.M., Merbold, L., Beier, C., McDowell, N.,
1036 Dukes, J.S.: Experiments to confront the environmental extremes of climate change, *Front. Ecol.*
1037 *Environ.*, 13, 219-225, doi: 10.1890/140174, 2015.
- 1038
- 1039 Keenan, T.F., Darby, B., Felts, E., Sonnentag, O., Friedl, M., Hufkens, K., O’Keefe, J.,
1040 Klosterman, S., Munger, J.W., Toomey, M., Richardson, A.D.: Tracking forest phenology and
1041 seasonal physiology using digital repeat photography: a critical assessment. *Ecol. Appl.*, 24,
1042 1478-1489. doi: <http://dx.doi.org/10.1890/13-0652.1>, 2014.
- 1043
- 1044 Kimbal, B.A., Conley, M.M., Lewin, K.F.: Performance and energy costs associated with scaling
1045 infrared heater arrays for warming field plots from 1 to 100 m. *Theor. Appl. Climatol.*, 108, 247-
1046 265, 2012.
- 1047
- 1048 Kimball, B.A., Conley, M.M., Wang, S., Lin, X., Luo, C., Morgan, J., Smith, D.: Infrared heater
1049 arrays for warming ecosystem field plots, *Global Change Biol.*, 14, 309-320. doi:
1050 10.1111/j.1365-2486.2007.01486.x, 2008.
- 1051
- 1052 Kimball, B.A.: Comment on the comment by Amthor et al. on “Appropriate experimental
1053 ecosystem warming methods” by Aronson and McNulty. *Agric. For. Meteorol.*, **151**, 420-424,
1054 2011.



- 1055
- 1056 Kolka, R.K., Sebestyen, S.D., Verry, E.S., Brooks, K.N.: *Peatland biogeochemistry and*
1057 *watershed hydrology at the Marcell Experimental Forest*, CRC Press, Boca Raton, 488 p, 2011.
- 1058
- 1059 Krassovski, M.B., Riggs, J.S., Hook, L.A., Nettles, W.R., Boden, T.A., Hanson, P.J.: A
1060 comprehensive data acquisition and management system for an ecosystem-scale peatland
1061 warming and elevated CO₂ experiment, *Geosci. Instrumen. Meth, Data Sys.*, 4, 203–213,
1062 doi:10.5194/gi-4-203-2015, 2015.
- 1063
- 1064 Kupper, P., Söber, J., Sellin, A., Löhmus, K., Tullus, A., Räm, O., Lubenets, K., Tulva, I., Uri,
1065 V., Zobel, M., Kull, O., Söber, A.: An experimental facility for free humidity manipulation
1066 (FAHM) can alter water flux through deciduous tree canopy, *Environ. Exper. Bot.*, 72, 432-438,
1067 2011.
- 1068
- 1069 LeCain, D., Smith, D., Morgan, J., Kimball, B.A., Pendall, E., Miglietta, F.: Microclimatic
1070 Performance of a Free-Air Warming and CO₂ Enrichment Experiment in Windy Wyoming,
1071 USA, *PLoS ONE*, 10, e0116834. doi:10.1371/journal.pone.0116834, 2015.
- 1072
- 1073 Leuzinger, S., Fatichi, S., Cusens, J., Körner, C., Niklaus, P.A.: The ‘island effect’ in terrestrial
1074 global change experiments: a problem with no solution? *AoB Plants*, 7, plv092, doi:
1075 10.1093/aobpla/plv092, 2015.
- 1076
- 1077 Medhurst, J., Parsby, J., Linder, S., Wallin, G., Ceschia, E., Slaney, M.: A whole-tree chamber
1078 system for examining tree-level physiological responses of field-grown trees to environmental
1079 variation and climate change, *Plant Cell Environ.*, 29, 1853-1869, 2006.
- 1080
- 1081 Medlyn, B.E., Zaehle, S., De Kauwe, M.G., Walker, A.P., Dietze, M.C., Hanson, P.J., Hickler,
1082 T., Jain, A.K., Luo, Y., Parton, W., Prentice, I.C., Thornton, P.E., Wang, S., Wang, Y-P., Weng,
1083 E., Iversen, C.M., McCarthy, H.R., Warren, J.M., Oren, R., Norby, R.J.: Using ecosystem
1084 experiments to improve vegetation models, *Nature Clim. Change*, 5, 528-534 DOI:
1085 10.1038/NCLIMATE2621, 2015.



- 1086
- 1087 Natali, S.M., Schuur, E.A.G., Trucco, C., Hicks Pries, C.E., Crummer, K.G., Baron Lopez, A.F.:
- 1088 Effects of experimental warming of air, soil and permafrost on carbon balance in Alaskan tundra,
- 1089 *Global Change Biol.*, 17, 1394-1407, 2011.
- 1090
- 1091 Norby, R.J., Edwards, N.T., Riggs, J.S., Abner, C.H., Wullschleger, S.D., Gunderson, C.A.:
- 1092 Temperature-controlled open-top chambers for global change research. *Global Change Biol.*, 3,
- 1093 259-267, 1997.
- 1094
- 1095 O’Gorman, E.J., Benstead, J.P., Cross, W.F., Friberg, N., Hood, J.M., Johnson, P.W.,
- 1096 Sigurdsson, B.D., Woodward, G.: Climate change and geothermal ecosystems: natural
- 1097 laboratories, sentinel systems, and future refugia, *Global Change Biol.*, 20, 3291-3299, doi:
- 1098 10.1111/gcb.12602, 2015.
- 1099
- 1100 Parsekian, A.D., Slater, L., Ntarlagiannis, D., Nolan, J., Sebestyen, S.D., Kolka, R.K., Hanson,
- 1101 P.J.: Uncertainty in peat volume and soil carbon estimated using ground-penetrating radar and
- 1102 probing, *Soil Sci. Soc. Amer. J.*, 76, 1911-1918, doi: 10.2136/sssaj2012.0040, 2012.
- 1103
- 1104 Petach, A.R., Toomey, M., Aubrecht, D.M., Richardson, A.D.: Monitoring vegetation phenology
- 1105 using an infrared-enabled security camera, *Agric. For. Meteorol.*, 195-196, 143-151, doi:
- 1106 <http://dx.doi.org/10.1016/j.agrformet.2014.05.008>, 2014.
- 1107
- 1108 Oleson, K.W., Lawrence, D.M., et al.: *Technical Description of version 4.5 of the Community*
- 1109 *Land Model (CLM)*. National Center for Atmospheric Research, Boulder, Colorado, NCAR/TN-
- 1110 503+STR NCAR Technical Note, July 2013, 2013.
- 1111
- 1112 Qi, Y., Heisler, G.M., Gao, W., Vogelmann, T.C., Bai, S.: Characteristics of UV-B Radiation
- 1113 Tolerance in Broadleaf Trees in Southern USA. Chapter 18 pp. 509-530, In: W. Gao, D. L.
- 1114 Schmoldt, JR Slusser, eds. *UV Radiation in Global Climate Change: Measurements, Modeling*
- 1115 *and Effects on Ecosystems*. Tsinghua University Press and Springer, 2010.
- 1116



- 1117 Raupach, M.R., Marland, G., Ciais, P., Le Queré, C., Canadell, J.G., Klepper, G., Field, C.B.:
1118 Global and regional drivers of accelerating CO₂ emissions. *Proc. Nat. Acad. Sci.*, 104, 10288-
1119 10293, 2007.
1120
- 1121 Rich, R.L., Stefanski, A., Montgomery, R.A., Hobbie, S.E., Kimball, B.A., Reich, P.B.: Design
1122 and performance of combined infrared canopy and belowground warming in B4WarmED
1123 (Boreal Forest Warming at an Ecotone in Danger) experiment, *Global Change Biol.*, **21**, 2334-
1124 2348, doi: 10.1111/gcb.12855, 2015.
1125
- 1126 Rustad, L.E., Campbell, J.L., Marion, G.M., Norby, R.J., Mitchell, M.J., Hartley, A.E.,
1127 Cornelissen, J.H.C., Gurevitch, J., GCTE-NEWS: A meta-analysis of the response of soil
1128 respiration, net nitrogen mineralization, and aboveground plant growth to experimental
1129 ecosystem warming, *Oecologia*, 126, 543–562, DOI 10.1007/s004420000544, 2001.
1130
- 1131 Sebestyen, S.D., Dorrance, C., Olson, D.M., Verry, E.S., Kolka, R.K., Elling, A.E., Kyllander,
1132 R.: Chapter 2: Long-term monitoring sites and trends at the Marcell Experimental Forest. In:
1133 Kolka RK, Sebestyen SD, Verry ES, Brooks KN (eds) *Peatland biogeochemistry and watershed*
1134 *hydrology at the Marcell Experimental Forest*. CRC Press, New York, pp 15-72, 2011.
1135
- 1136 Sebestyen, S.D., Griffiths, N.A.: *SPRUCE Enclosure Corral and Sump System: Description,*
1137 *Operation, and Calibration*. Climate Change Science Institute, Oak Ridge National Laboratory,
1138 U.S. Department of Energy, Oak Ridge, Tennessee, U.S.A,
1139 <http://dx.doi.org/10.3334/CDIAC/spruce.030>, 2016.
1140
- 1141 Shaver, G.R., Canadell, J., Chapin, F.S. III: Global warming and terrestrial ecosystems: a
1142 conceptual framework for analysis, *Biosci*, 50, 871–882, 2000.
1143
- 1144 Shi, X., Thornton, P.E., Ricciuto, D.M., Hanson, P.J., Mao, J., Sebestyen, S.D., Griffiths, N.A.,
1145 Bisht, G.: Representing northern peatland microtopography and hydrology within the
1146 Community Land Model, *Biogeosciences*, 12, 6463-6477, doi:10.5194/bg-12-6463-2015, 2015.
1147



- 1148 Strack, M.: *Peatlands and Climate Change*. International Peat Society. Jyväskylä, Finland, 223
1149 p, 2008.
1150
- 1151 Tfaily, M.M., Cooper, W.T., Kostka, J., Chanton, P.R., Schadt, C.W., Hanson, P.J., Iversen,
1152 C.M., Chanton, J.P.: Organic matter transformation in the peat column at Marcell Experimental
1153 Forest: humification and vertical stratification, *JGR–Biogeosciences*, 119, 661–675,
1154 doi:10.1002/2013/JG002492, 2014.
1155
- 1156 Toomey, M., Friedl, M.A., Frohling, S., Hufkens, K., Klosterman, S., Sonnentag, O., Baldocchi,
1157 D.D., Bernacchi, C.J., Biraud, S.C., Bohrer, G., Brzostek, E., Burns, S.P., Coursolle, C.,
1158 Hollinger, D.Y., Margolis, H.A., McCaughey, H., Monson, R.K., Munger, J.W., Pallardy, S.,
1159 Phillips, R.P., Torn, M.S., Wharton, S., Zeri, M., Richardson, A.D.: Greenness indices from
1160 digital cameras predict the timing and seasonal dynamics of canopy-scale photosynthesis, *Ecol.*
1161 *Appl.*, 25, 99–115. <http://dx.doi.org/10.1890/14-0005.1>, 2015.
1162
- 1163 Torn, M.S., Chabbi, A., Crill, P., Hanson, P.J., Janssens, I.A., Luo, Y., Hicks Pries, C., Rumpel,
1164 C., Schmidt, M.W.I., Six, J., Schrumpf, M., Zhu, B.: A call for international soil experiment
1165 networks for studying, predicting, and managing global change impacts, *Soil*, 1, 575–582, 2015.
1166 Verry, E.S., Brooks, K.N., Barten, P.K.: Streamflow response from an ombrotrophic mire. In:
1167 Symposium on the hydrology of wetlands in temperate and cold regions. Publications of the
1168 Academy of Finland, Helsinki, pp 52–59, 1988.
1169
- 1170 Walther, G.-R., Post E., Convey, P., Menzel, A., Parmesan, C., Beebee, T.J.C., Fromenten, J-
1171 M., Hoegh-Guldberg, O., Bairlein, F.: Ecological responses to recent climate change, *Nature*,
1172 416, 389–395, 2002.
1173